CHAPTER TEN

Folds and Folding

10.1 INTRODUCTION

Ask a structural geologist, or any other geologist for that matter, about their favorite structure and chances are that they will choose folds. If you have seen a fold in the field you will have marveled at its appearance (Figure 10.1). Let's face it, it is pretty unbelievable that hard rocks are able to change shape in such a dramatic way. In simple terms, a fold is a structural feature that is formed when planar surfaces are bent or curved. If such surfaces (like bedding, cleavage, inclusions) are not available you will not see a fold even though the rock was deformed. Folding is a manifestation of ductile deformation because it can develop without fracturing, and the deformation is (heterogeneously) distributed over the entire structure. Rather than fracturing, processes such as grain sliding, kinking, dissolution, and crystal plasticity dominate. Looking at a fold from a kinematic perspective, you realize that strain in this structure cannot be the same everywhere. We recognize distinct segments in a fold, such as the hinge area and the limbs, the inner and the outer arc, each of which reflect different strain histories, regardless of scale.

Why do folds exist, how do rocks do it, and what does folding mean for regional analysis? These and other questions were first asked quite some time ago and much of what we know today about folds and folding was well established before the 1980s. The geometry of folds tells us something about, for example, the degree and orientation of strain, which in turn provides critical information about the deformation history of a region. Much of the work in recent years represents refinements of some of the earlier work; we can apply increasingly sophisticated numerical and experimental approaches. Yet, the fundamental observations remain essentially intact. Therefore, in this chapter we will mainly look at some of the first principles of folding

FIGURE 10.1 Large-scale recumbent fold in the Caledonides of northeast Greenland. The height of the cliff is about 800 m and the view is to the Northwest. *(Kildedalen)*

and their application to structural analysis. First, however, we discuss the basic vocabulary needed to communicate about folds and fold systems.

10.2 ANATOMY OF A FOLDED SURFACE

The schematic illustration in Figure 10.2 shows the basic geometric elements of a fold. The **hinge area** is the region of greatest curvature and separates the two limbs. The line of greatest curvature in a folded surface is called the **hinge line.** You may think of a **limb** as the less curved portion of a fold. In a limb there is a point where the sense of curvature changes, called the **inflection point.** Folds with a straight hinge line (Figure 10.3a) are called **cylindrical folds** when the folded

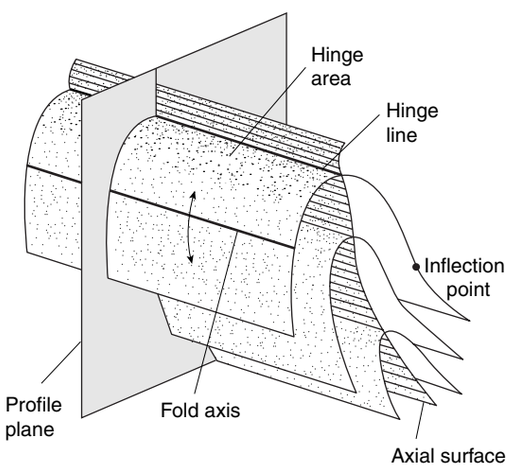

FIGURE 10.2 The terminology of a fold.

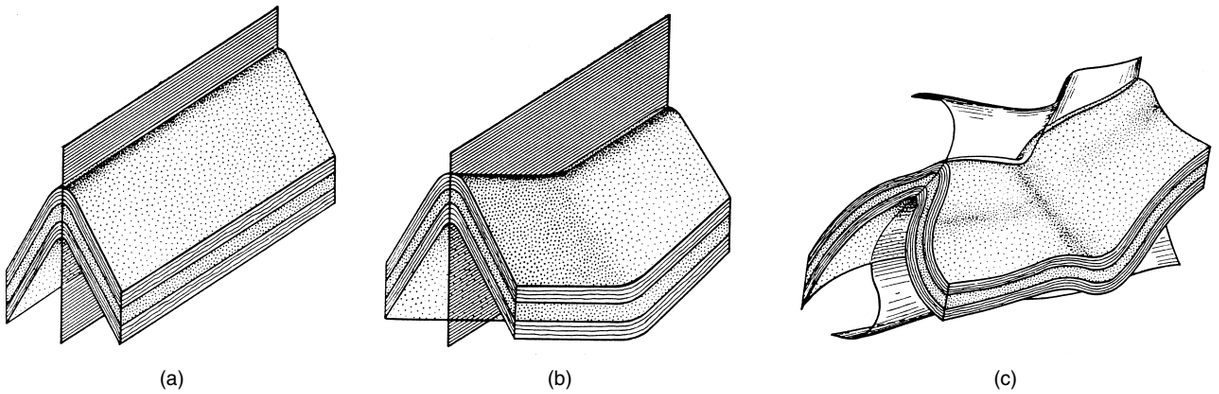

FIGURE 10.3 A cylindrical fold (a) is characterized by a straight hinge line and a noncylindrical fold (b) by a curved hinge line. The axial surface may be planar, as in (a) and (b), or curved (c).

surface can wrap partway around a cylinder. If this is not the case and the hinge line curves, the folds are called **noncylindrical** (Figure 10.3b). In reality the lateral extent of cylindrical folds is restricted to the outcrop scale or even less, because over greater distances the hinge line of folds typically curves. Nevertheless you will find that we may conveniently treat natural folds as cylindrical by dividing them into segments with straight hinge lines.

A cylindrical surface consists of an infinite number of lines that are parallel to a generator line. This generator line is called the **fold axis,** which, when moved parallel to itself through space, outlines the folded surface. In the case of cylindrical folds the fold axis is of course parallel to the hinge line.[1] The topographically highest and lowest points of a fold are called the **crest** and **trough,** respectively, and these do not necessarily coincide with hinge lines. The surface containing the hinge lines from consecutive folded surfaces in a fold is the **axial surface** (Figures 10.2 and 10.3). The term **axial plane** is loosely used by some, but the surface is not necessarily planar as seen in Figure 10.3c (recall the distinction between surface and plane). Moreover, the axial surface does not necessarily divide the fold into equal halves that are mirror images of one another. The reference plane used to describe fold shape is called the **fold profile plane,** which is perpendicular to the hinge line (Figure 10.2). Note that the profile plane is not the same as a cross section through the fold, which is any vertical plane through a body, much like the sides of a slice of layered cake. If the hinge line is not horizontal, then the profile plane is not parallel to the cross-sectional plane, which has implication for the fold geometry description.

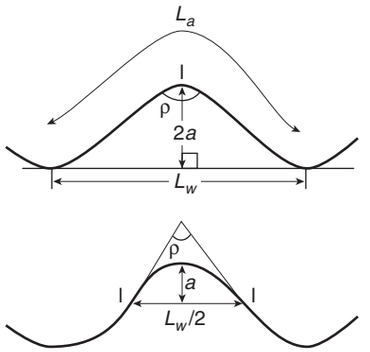

FIGURE 10.4 The interlimb angle (ρ), the wavelength (L_w), the amplitude (a), and the arc length (L_a) of a fold system in profile.

The angle between fold limbs as measured in the profile plane is called the **interlimb angle** (Figure 10.4). Intuitively you realize that the interlimb angle offers a qualitative estimate of the intensity of folding; the smaller the interlimb angle, the greater the intensity of folding. Finally, we recognize the **amplitude, wavelength,** and **arc length** of a fold in profile. These terms are used in the same manner as they are in wave physics, because folds tend to look a bit like harmonic functions (such as a sine curve). The wavelength is defined as the distance between two hinges of the same orientation, while the arc length is this distance measured over the folded surface; the amplitude is half the height of the structure measured from crest to trough (Figure 10.4). These and other terms associated with folds are summarized in Table 10.1.

When successive layers in a folded stack have approximately the same wavelength and amplitude, the

[1]Sometimes fold axis is used as a synonym for hinge line, but this is not correct.

TABLE 10.1 VOCABULARY OF A FOLD

Amplitude	Half the height of the structure measured from crest to trough
Arc length	The distance between two hinges of the same orientation measured over the folded surface
Axial surface	The surface containing the hinge lines from consecutive folded surfaces
Crest	The topographically highest point of a fold, which need not coincide with the fold hinge
Cross section	A vertical plane through a fold
Culmination	High point of the hinge line in a noncylindrical fold
Cylindrical fold	Fold in which a straight hinge line parallels the fold axis; in other words, the folded surface wraps partway around a cylinder
Depression	Low point of the hinge line in a noncylindrical fold
Fold axis	Fold generator in cylindrical folds
Hinge	The region of greatest curvature in a fold
Hinge line	The line of greatest curvature
Inflection point	The position in a limb where the sense of curvature changes
Limb	Less curved portion of a fold
Noncylindrical fold	Fold with a curved hinge line
Profile plane	The surface perpendicular to the hinge line
Trough	The topographically lowest point of a fold, which need not coincide with the fold hinge
Wavelength	The distance between two hinges of the same orientation

folds are called **harmonic.** If some layers have different wavelengths and/or amplitudes, the folds are **disharmonic** (Figure 10.5). In extreme circumstances, a series of folded layers may be totally decoupled from unfolded layers above or below. When this happens, a **detachment** horizon exists between folded and unfolded layers.

10.2.1 Fold Facing: Antiform, Synform, Anticline, and Syncline

Take a deep breath. We have already sprung a sizable array of terms on you, but before we explore the significance of folding, we have yet to add a few more. Maybe you will find comfort in the knowledge that generations of students before you have plowed their way through this terminology, happily discovering that in the end it really is important for the description and interpretation of regional deformation. Having said this, now draw a fold on a piece of paper. Chances are that you place the hinge area at the top of the structure, outlining something like a sharp mountain. In fact, a psychological study among geologists found this invariably to be true (just look at your neighbor's sketch).[2] This particular fold geometry is called an **antiform.** The opposite geometry, when the hinge zone is at the bottom (outlining a valley), is called a **synform.** The explanation for the modifiers "anti" and "syn" is that the limbs dip away from or toward the center of the fold, respectively. You will find that many geologists use the terms anticline and syncline as synonyms for antiform and synform, but this is incorrect. The terms anticline and syncline imply that the stratigraphic younging direction in the folded beds is known. This is an important distinction for regional analysis, so let's look at this in some detail.

Imagine a sequence of beds that is laid down in a basin over a period of many millions of years. Obviously, the youngest bed lies at the top while the oldest bed is at the bottom of the pile (this is Steno's **Law of Superposition**). When we fold this sequence into a

[2]This is not (yet) linked to any criminal behavior.

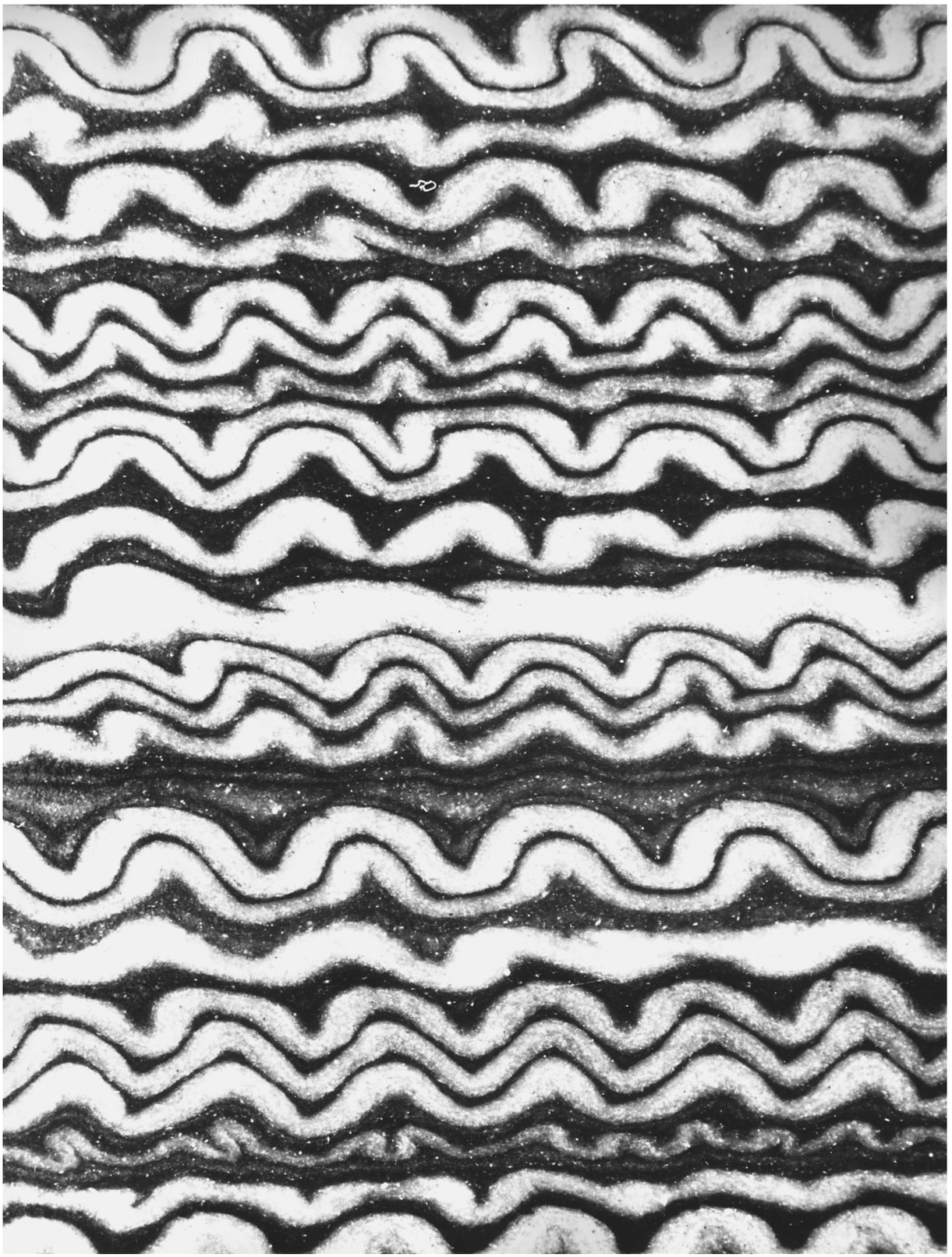

FIGURE 10.5 Small-scale disharmonic folds in anhydrite of the Permian Castile Formation in the Delaware Basin of Texas. White layers are anhydrite; dark layers consist of calcite that is rich in organic material (hence the dark color). Note that detachments occur in the organic-rich calcite layers and that the fold shapes (including box folds) in the anhydrite vary as a function of layer thickness.

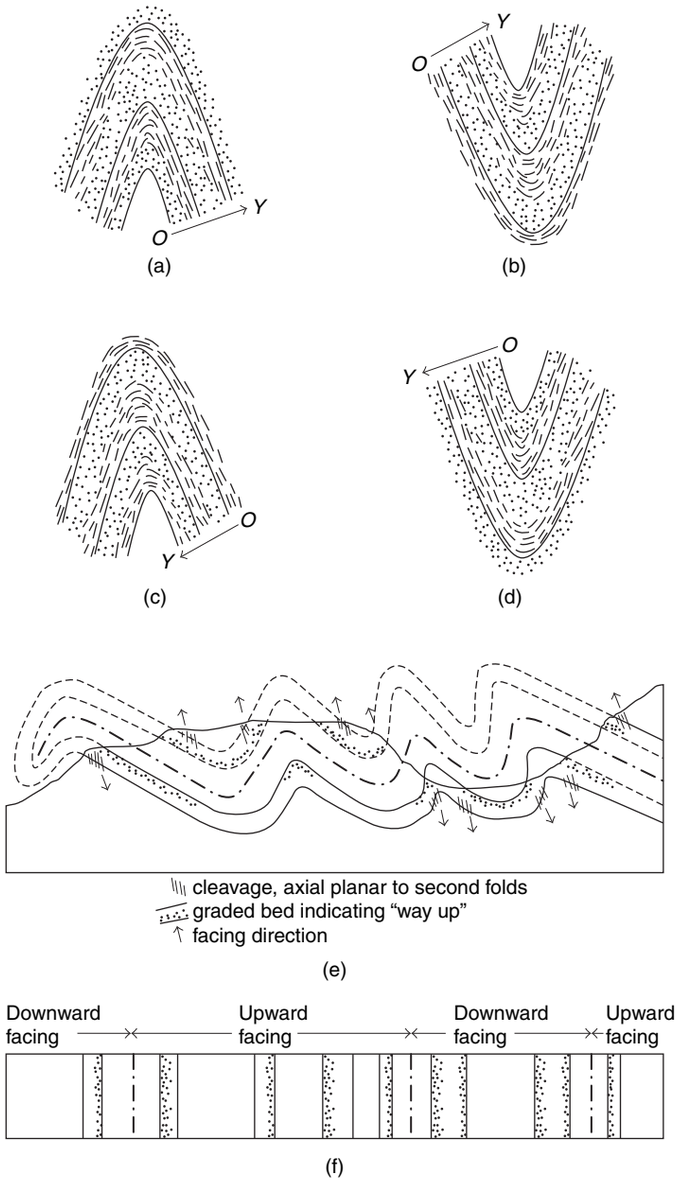

FIGURE 10.6 Antiforms, synforms, and fold facing. An upward-facing antiform (a) is also called an anticline and an upward-facing synform (b) is called a syncline. Downward-facing antiforms (c) and downward-facing synforms reflect an early history that placed the beds upside down prior to folding. These forms may occur in a region containing two generations of folding (e). The corresponding facing in map view across this area is shown in (f). Younging direction is indicated by $O \rightarrow Y$ arrow.

series of antiforms and synforms, we see that the oldest bed lies in the core of the antiform and the youngest bed lies in the core of the synform (Figure 10.6a and 10.6b). Under these circumstances we call them anticlines and synclines, respectively. In an **anticline** the beds young away from the core; in a **syncline** the beds young toward the core. In both cases the younging direction points (or faces) upward, so we call these structures **upward-facing folds.** Now turn the original sequence upside down: the oldest bed now lies at the top and the youngest bed at the bottom (Figure 10.6c and 10.6d). While we generate the same geometry of antiforms and synforms, the younging direction is opposite to what we had before. In this antiform, the beds young toward the core, while in the synform the beds young away from the core. Both cases are **downward-facing folds,** and an antiform with this younging characteristic is therefore called a **downward-facing antiform;** analogously, we recognize a **downward-facing synform.**[3] Remember that when you find downward-facing folds in the field, you immediately know that some secondary process has inverted the normal stratigraphic sequence; that is, we cannot violate the Law of Superposition. Downward-facing folds are not as uncommon as one might guess. They are typically found in areas containing an early "generation" of regional folds with horizontal axial surfaces, which are quite common in collisional mountain belts. Subsequent folding of these early structures generates a series of upward- and downward-facing folds, as shown in Figure 10.6e. But we must not get ahead of ourselves; the principle of superposed folding is discussed in a later section of this chapter.

10.3 FOLD CLASSIFICATION

Now that we have established a basic vocabulary we can further classify folds. The classification of folds is based on four components:

1. Fold shape in three dimensions, primarily distinguishing between cylindrical folds and noncylindrical folds (Figure 10.3).
2. Fold facing, separating upward-facing folds and downward-facing folds (Figure 10.6).
3. Fold orientation.
4. Fold shape in the profile plane.

The first two components, three-dimensional fold shape and fold facing, have already been introduced (Figures 10.3 and 10.6, respectively). In this section

[3]The antiform and synform have the younging characteristics of a syncline and anticline, respectively, and are therefore also called *antiformal syncline* and *synformal anticline,* respectively.

FIGURE 10.7 An asymmetric, plunging fold (the Sheep Mountain Anticline in Wyoming, USA).

we concentrate on the other two components of fold classification: fold orientation and fold shape.

10.3.1 Fold Orientation

Looking at the curved surface of a natural fold makes one wonder if there is any one representative measurement for the structure (Figure 10.7). Taking your compass to the folded surface will give you a large number of different readings for dip, and dip and strike (or dip direction) if the fold is noncylindrical. In folds with limbs that are relatively straight, you will find that all the measurements in a single limb are pretty much alike (Figure 10.8), but in folds with curving limbs this will not be the case. So what do we measure if we want to give the orientation of a fold to another geologist? The first measurement we take is the orientation of the hinge line (Figure 10.9). On the scale of an outcrop the hinge line is typically fairly straight, and we determine its plunge (say, 20°) and direction of plunge (say, 190°). We now say that the fold is shallowly plunging to the South. Secondly, we measure the orientation of the axial surface. We measure a dip direction/dip of 270°/70° for the axial surface, which completes our description of the fold: *a shallowly south-plunging, upright fold.* Remember that the hinge line always lies in the axial surface. Test your measurements in a spherical projection to see whether this relationship holds. What constrains terms like **shallow** and **upright?** As a practical convention we use the angular ranges shown in Table 10.2.

In Figure 10.10 we show some representative combinations of hinge line and axial surface orientations with their terminology. A fold with a horizontal axial surface by definition must have a horizontal hinge line, and is called a **recumbent fold** (Figure 10.1). In the European Alps, for example, large-scale recumbent

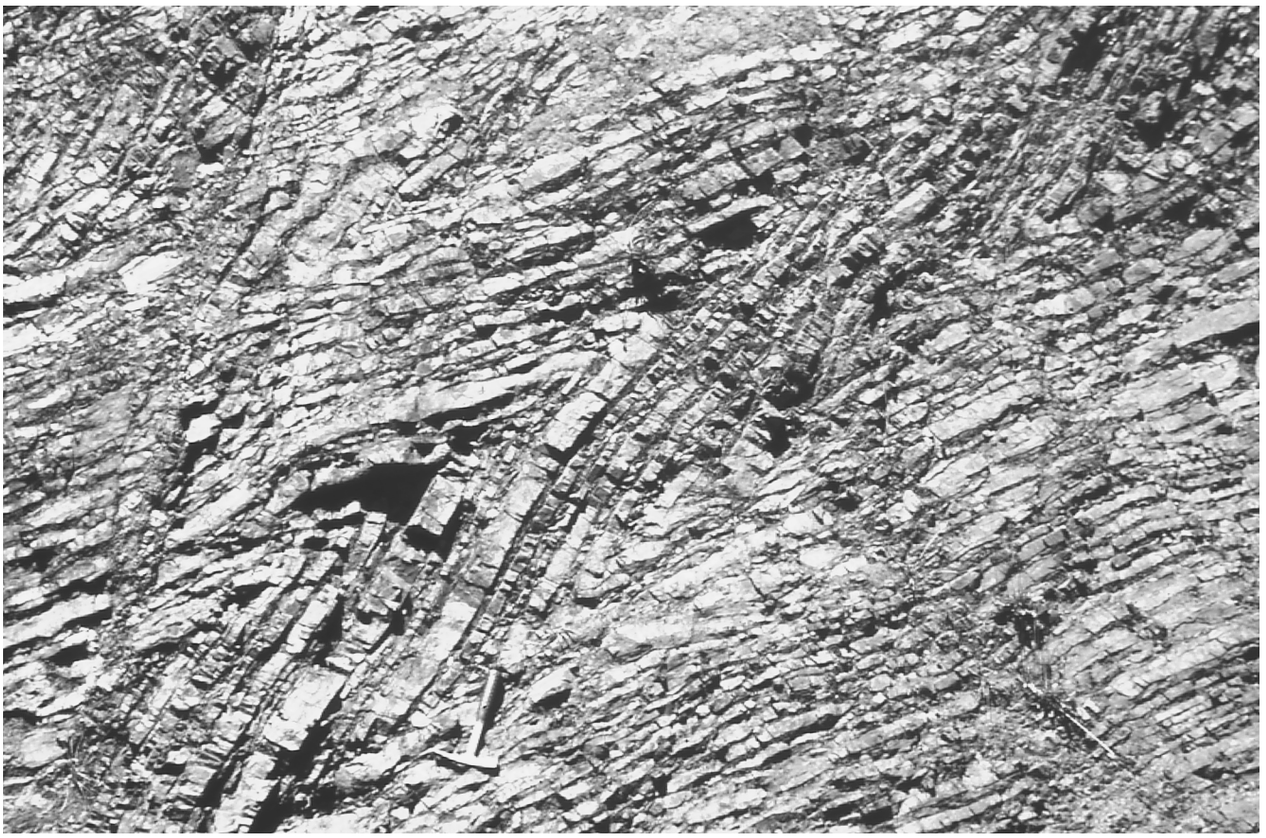

FIGURE 10.8 Chevron folds in Franciscan chert of California, USA (Marin County).

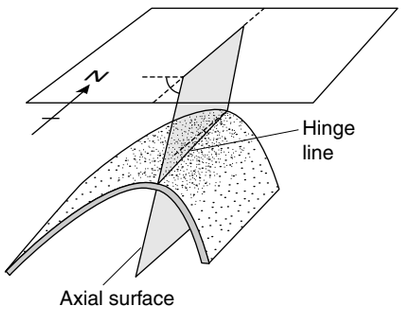

FIGURE 10.9 Fold orientation. Note that the axial surface is a *plane* whose orientation is given by dip and strike (or dip direction), whereas the hinge is a *line* whose orientation is given by plunge and bearing.

folds are often associated with thrust faulting, and they are called **nappes** (see Figure 9.1). A term that is used for a steeply plunging, inclined fold is a **reclined fold.** In all cases remember that your field measurements will be no more accurate than ±2° (compass accuracy), but that the feature you measure will probably vary over an even greater angle of ±5°–10°. Thus, the values in Table 10.2 serve as a guide and should not be applied too strictly; they are not carved in stone.

TABLE 10.2 FOLD CLASSIFICATION BY ORIENTATION

Plunge of Hinge Line	Dip of Axial Surface
Horizontal: 0°–10°	Recumbent: 0°–10°
Shallow: 10°–30°	Inclined: 10°–70°
Intermediate: 30°–60°	Upright: 70°–90°
Steep: 60°–80°	
Vertical: 80°–90°	

10.3.2 Fold Shape in Profile

The profile plane of a fold is defined as the plane perpendicular to the hinge line (Figure 10.2). The fold shape in profile (as viewed, by convention, down the plunge) allows further classification of folds. Because the profile plane is perpendicular to the hinge line, we need not concern ourselves with the orientation of the fold. Fold shape in profile describes the interlimb angle and any changes in bed thickness. The *interlimb*

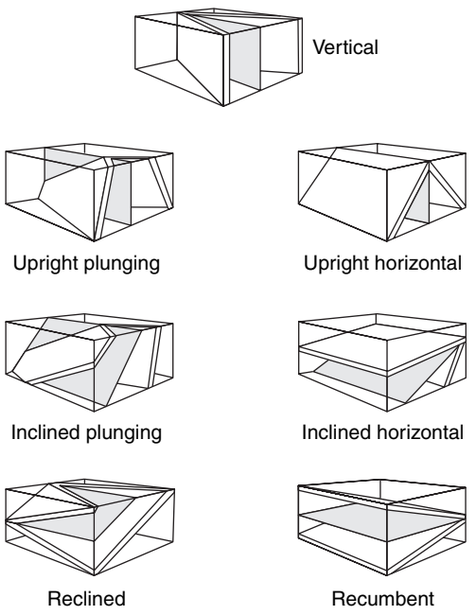

FIGURE 10.10 Fold classification based on the orientation of the hinge line and the axial surface (shaded).

angle of a fold is the angle between the limbs. We assume that the limbs are relatively planar or we use the tangent at the inflection points (Figure 10.4). The values corresponding to the various terms are listed in Table 10.3. As with those in Table 10.2, they serve only as a rough guide.

The second characteristic of fold shape in profile is any change in *bed thickness* across the structure. If you look at Figure 10.11a, you will notice that the bed thickness does not change appreciably as we go from one limb of the fold to the other. In contrast, the fold in Figure 10.11b has thin limbs and a relatively thick hinge area. We quantify these observations by using a method called **dip-isogon analysis.** Dip isogons connect points on the upper and lower boundary of a folded layer where the layers have the same dip relative to a reference frame (Figure 10.12). The construction method is explained step by step in all structural geology laboratory manuals, to which you are referred.[4] Three classes are recognized: **convergent dip isogons** (Class 1), **parallel dip isogons** (Class 2), and **divergent dip isogons** (Class 3). The terms "convergence" and "divergence" are used with respect to the core of the fold;[5] when the dip isogons intersect in a point in the core of the fold, the fold is called convergent, and vice versa. The two geometries shown in Figure 10.11 are special cases. Dip isogons that are perpendicular to bedding throughout the fold define a **parallel fold,** whereas dip isogons that are parallel to each other characterize a **similar fold.** This terminology (especially the use of "parallel") may be confusing, but remember that parallel and similar describe the geometric relationship between the top and bottom surfaces of a folded layer; they do not describe the relationship between individual dip isogons in a fold. Parallel and similar folds anchor the finer fivefold subdivision that is used mainly for detailed description. In the field, loosely using the terms similar (representing Class 2 and 3) and parallel (representing Class 1A, 1B, and 1C) is usually sufficient to describe the fold shape in profile.

TABLE 10.3 **FOLD CLASSIFICATION BY INTERLIMB ANGLE**

Isoclinal	0°–10°
Tight	10°–60°
Open	60°–120°
Gentle	120°–180°

So we added two more components to our description of a fold. Now as a test, sketch a shallowly plunging, upright, tight, similar, downward-facing synform in the margin of the text. Hopefully these terms have become sufficiently clear that the task, unlike its description, is relatively simple. The only parameter we have excluded in our classification is **fold size.** To specify this we can use terms like microfold (microscopic size; up to millimeter scale), mesofold (hand specimen to small outcrop size; centimeter to meter scale), and macrofold (mountain size and larger; hundreds to thousands of meters). Although the lengthy description above is certainly not pretty, it ends up being very informative and complete. Remember that the goal of any good description is first to recall the characteristics for yourself, and secondly to relay this information in an understandable and unequivocal fashion to someone else.

10.4 FOLD SYSTEMS

Our treatment of folds so far has concentrated mostly on single antiforms and synforms. When we have a series of antiforms and synforms, we call this a **fold**

[4]Graphically, the dip isogon classification plots angle α versus normalized distance between the two tangents defining a dip isogon.

[5]The same terminology returns with cleavage (Chapter 12).

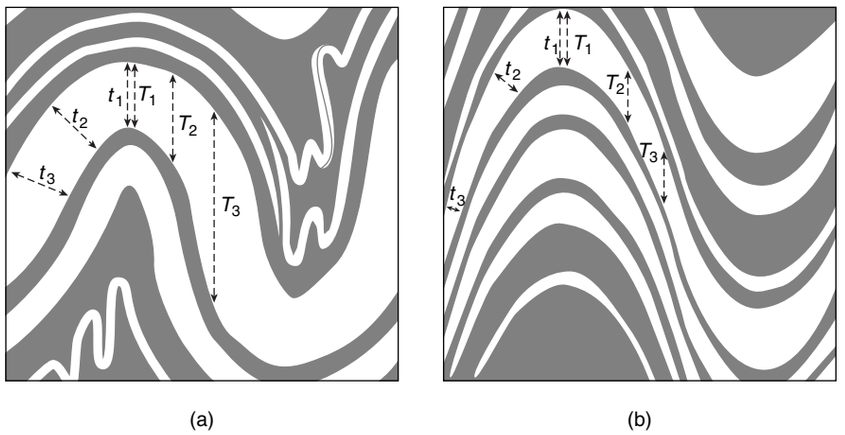

FIGURE 10.11 Parallel folds (a) maintain a constant layer thickness across the folded surface, meaning, $t_1 = t_2 = t_3$, but the layer thickness parallel to the axial surface varies ($T_1 < T_2 < T_3$). Note that parallelism must eventually break down in the cores of folds because of space limitation, which is illustrated by the small disharmonic folds in (a). In similar folds (b), the layer thickness parallel to the axial surface remains constant, so, $T_1 = T_2 = T_3$, but the thickness across the folded surface varies ($t_1 > t_2 > t_3$). Similar folds do not produce the space problem inherent in parallel folds.

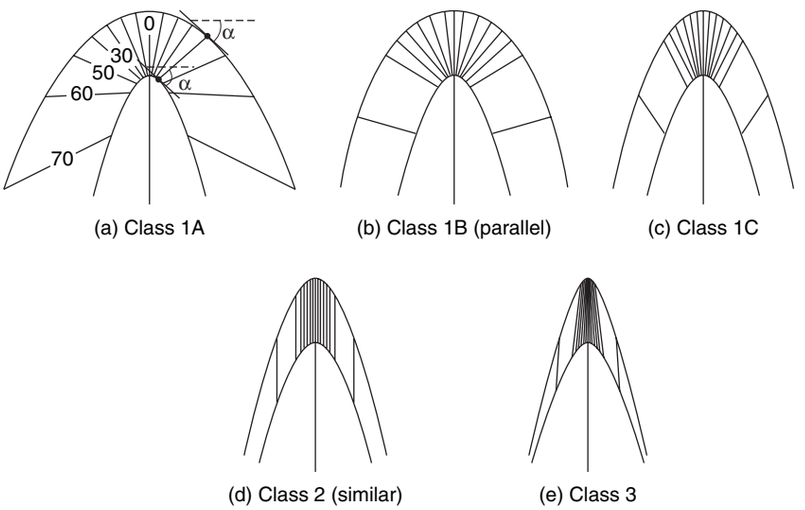

FIGURE 10.12 Fold classification based on dip isogon analysis. In Class 1A (a) the construction of a single dip isogon is shown, which connects the tangents to the upper and lower boundary of the folded layer with equal angle (α) relative to a reference frame; dip isogons at 10° intervals are shown for each class. Class 1 folds (a–c) have convergent dip isogon patterns; dip isogons in Class 2 folds (d) are parallel; Class 3 folds (e) have divergent dip isogon patterns. In this classification, parallel (b) and similar (d) folds are labeled as Class 1B and Class 2, respectively.

system. The information we can obtain from fold systems provides some of the most powerful information for the interpretation of regional structure, and involves such elements as fold symmetry, fold vergence, and the enveloping surface. We start with the last of these.

10.4.1 The Enveloping Surface

Draw an imaginary plane that is tangential to the hinge zones of a series of small folds in a layer (surface *A*, Figure 10.13). We call this surface the **enveloping surface.** It contains all the antiformal or synformal hinges.[6] Figure 10.13 also shows that we can draw an additional enveloping surface (surface *B*) when we connect the hinges of the curved enveloping surface *A*. We call the enveloping surface for the largest folds the first-order enveloping surface (here surface *B*). The enveloping surfaces of successively smaller structures have a higher order (second-order enveloping surface, third-order enveloping surface, and so on). The first-order enveloping surface is typically of regional scale, while higher-order enveloping surfaces may go down as low as the thin-section scale. But what is the point of determining the enveloping surface? With decreasing order, the enveloping surfaces reduce the structural information of a folded area into increasingly simple patterns. For example, the second-order enveloping surface in Figure 10.13 shows that the small-scale folds define a larger-scale fold pattern consisting of antiforms and synforms. These large-scale structures have also been designated by the terms **anticlinorium** and **synclinorium,** respectively. Unfortunately the use of these terms suggests upward-facing structures, which is not

[6]In the case of folds with horizontal or shallowly dipping axial surfaces, we refer to these as crests and troughs, respectively.

always intended. The presence of anticlinoria and synclinoria implies that many small folds are somehow related, even though they vary in shape and position in the larger structure. It is important to realize that the orientations of these small folds (both hinge line and axial surface) are often the same, and also that these parameters approximately parallel that of the anticlinorium and synclinorium. For that reason, these small folds are sometimes called **parasitic folds,** because they are related to a larger structure.

The geometric relationship between parasitic folds and regional structures offers a powerful concept in structural analysis, which states that the orientation of small (high-order) structures is representative of the orientation of regional (low-order) structures.[7] Thus, the orientations of the hinge line and the axial surface of a small fold can predict these elements for a large regional fold that is otherwise not exposed; in Figure 10.13 you indeed see that this is the case. Obviously, this "rule" serves only as a convenient working hypothesis, but it has proven to be very robust in regional mapping. Use this rule on a field trip and surprise friend and foe with your quick insight into regional structure.

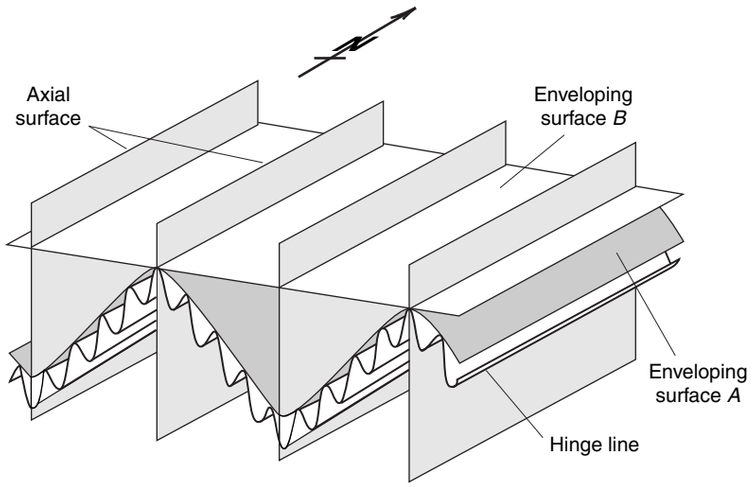

FIGURE 10.13 The enveloping surface connects the antiform (or synform) hinges of consecutive folds (surface *A*). If this imaginary surface appears to be folded itself, we may construct yet a higher-order enveloping surface (surface *B*). Note that the orientations (hinge line and axial surface) of the small folds and the large-scale folds are very similar.

10.4.2 Fold Symmetry and Fold Vergence

The relationship between the enveloping surface and the axial surface of folds also enables us to describe the symmetry of folds. If the enveloping surface and the axial surface are approximately perpendicular (±10°), we have **symmetric folds** (Figure 10.14a); otherwise the folds are **asymmetric** (Figure 10.14b). In the case of an isolated fold, an enveloping surface cannot be defined. To determine if a fold is symmetric or asymmetric we use the median surface, which is the surface that passes through the inflection points of opposing limbs. If the axial surface is perpendicular to the median surface, then the fold is symmetric; otherwise the fold is asymmetric. There are other definitions of fold symmetry that involve, for example, the relative steepness of limbs, but these descriptions of fold symmetry are often ambiguous and should not be used.

Now let's look at a practical application of fold symmetry. The second-order enveloping surface defined by the small folds of Figure 10.13 outlines a large antiform-synform pair. The small folds (the *parasitic folds*) show characteristic shapes and asymmetries as we move along the second-order enveloping surface. On the west limb of the large antiform, the minor folds are asymmetric and have what we call a clockwise asymmetry when looking down the plunge of the fold. In the hinge area, the folds are symmetrical, because the axial surface is perpendicular to the enveloping surface. In fact, as we move from the limb toward the hinge area, the clockwise asymmetry becomes progressively less, until the fold is symmetrical. As we move into the east limb of the antiform, the fold asymmetry returns, but now with the opposite sense to that in the west limb; in the east limb the asymmetry is counterclockwise. Note that clockwise and counterclockwise

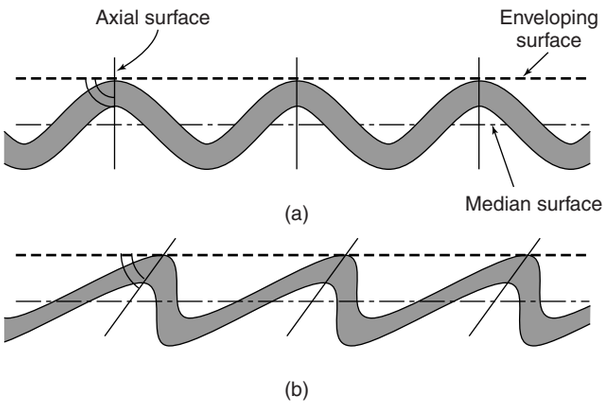

FIGURE 10.14 Symmetric (a) and asymmetric folds (b) are defined by the angular relationship between the axial surface and the enveloping surface.

[7]This is otherwise known as *Pumpelly's Rule,* after the nineteenth-century American geologist Raphael Pumpelly.

are defined by the rotation of the axial surface relative to a hypothetical symmetrical fold (Figure 10.15). In the past, parasitic folds were erroneously given the genetic name "drag folds," because it was assumed that the apparent rotation of the axial surfaces reflects drag between the layers during folding. Rather, these minor folds are probably symmetrical in the incipient stages of regional folding and become more asymmetrical when the large folds tighten. So, across a large fold the **vergence**[8] of parasitic folds changes in a characteristic manner that allows us to predict the location of the hinge area of large antiforms and synforms (Figure 10.16). Using parasitic folds, we may even predict the orientation of these large regional folds (see previous section).

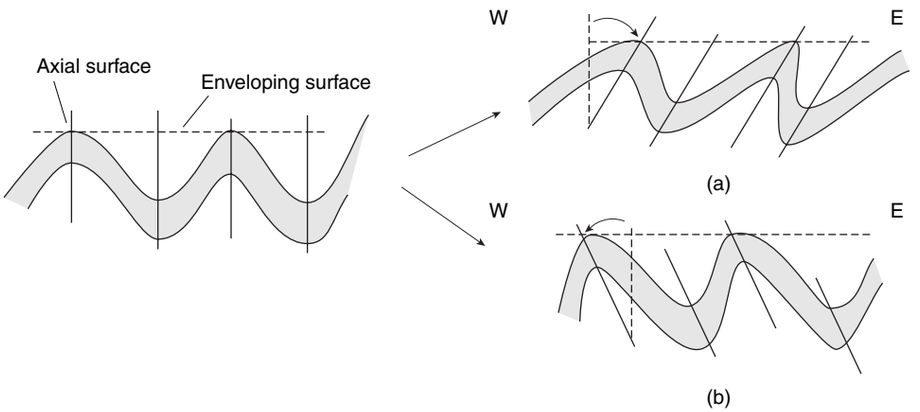

FIGURE 10.15 Fold vergence, clockwise (a) and counterclockwise (b), is defined by the apparent rotation of the axial surface from a hypothetical symmetric fold into the observed asymmetric fold, without changing the orientation of the enveloping surface. In a given geographic coordinate system we may also say east-verging (a) and west-verging (b) folds for clockwise and counterclockwise folds, respectively (for this example). In all descriptions we are looking down the plunge of the fold.

There is need for some caution when folds are not plunging; that is, in horizontal upright folds where down-plunge observations cannot be defined. If we view the structure in Figure 10.16 from the opposite side, the clockwise folds become counterclockwise (just hold the page with Figure 10.16 facing the light, viewing it from the back)! This situation is not as confusing as it seems at first. Imagine an antiform that is cut by a road perpendicular to the axial surface. The asymmetry of parasitic folds in this large structure appears clockwise or counterclockwise on opposite sides of the road. However, in both cases they make the same prediction for the location of the hinge area. As long as you define the direction in which you view the minor structure, there is no problem using fold vergence as a mapping tool in an area. A practical tip is to copy the geometry of Figure 10.16 into the back of your field notebook. Matching field observation with asymmetries in your sketch, which may require some rotation of your notebook, will ensure a reliable application of this mapping tool. In any case, remember that a pattern of fold vergence opposite to that in Figure 10.16 (a "Christmas-tree" geometry) cannot be produced in a single fold generation (Figure 10.17).[9]

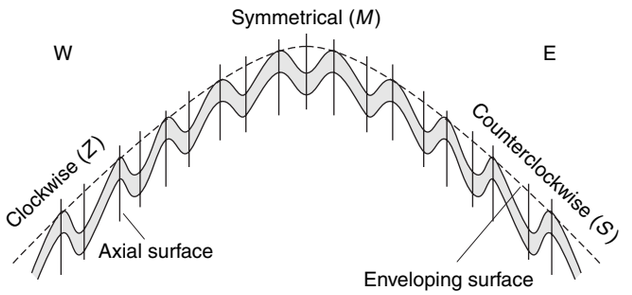

FIGURE 10.16 Characteristic fold vergence of parasitic folds across a large-scale antiform. Looking down the plunge, the parasitic fold changes from clockwise asymmetry (east-verging in the geographic coordinate system) to symmetric to counterclockwise asymmetry (west-verging) when going from W to E. You may also find that some geologists use the terms *Z*-, *M*-, and *S*-folds for this progression (for obvious reasons).

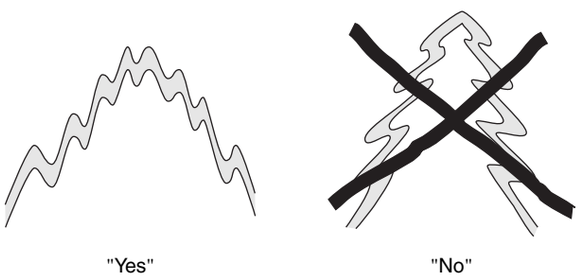

FIGURE 10.17 Right and wrong in fold vergence. It is useful to copy the images in Figures 10.16 and 10.17 in your field notebook for reference.

[8]Do not confuse fold vergence with fold facing.

[9]In fact, this geometry is diagnostic of the presence of at least two fold generations.

FIGURE 10.18 Monocline in the Big Horn Mountains (Wyoming, USA).

10.5 SOME SPECIAL FOLD GEOMETRIES

We end the descriptive part of this chapter with a few special fold geometries that you may encounter in your field career. **Monoclines** are fold structures with only one tilted limb; the beds on either side of the tilted limb are horizontal. Monoclines typically result from a vertical offset in the subsurface near the tilted portion of the structure. The fault uplifts a block of relatively rigid igneous or metamorphic rock, and the overlying sedimentary layers drape over the edge of the uplifted block to form the monocline (Figure 10.18). Spectacular examples are found in the Colorado Plateau of the western United States. **Kink folds** are small folds (less than a meter) that are characterized by straight limbs and sharp hinges. Typically they occur in finely laminated (that is, strongly anisotropic) rocks, such as shales and slates (Figure 10.19). Sharply bending a deck of cards is a good analogy for the kinking process, because kink folds are formed by displacements between individual laminae (individual cards in the analogy). **Chevron folds** (Figure 10.8) are the larger-scale equivalent of kink folds.

The term **box fold** describes a geometry that is pretty self-explanatory (Figure 10.5). In order for a box fold to form, a layer must be detached from the underlying and overlying layers. They are therefore common in areas with weak basal layers, such as in the Jura Mountains of Switzerland. **Ptygmatic folds** are irregular and isolated

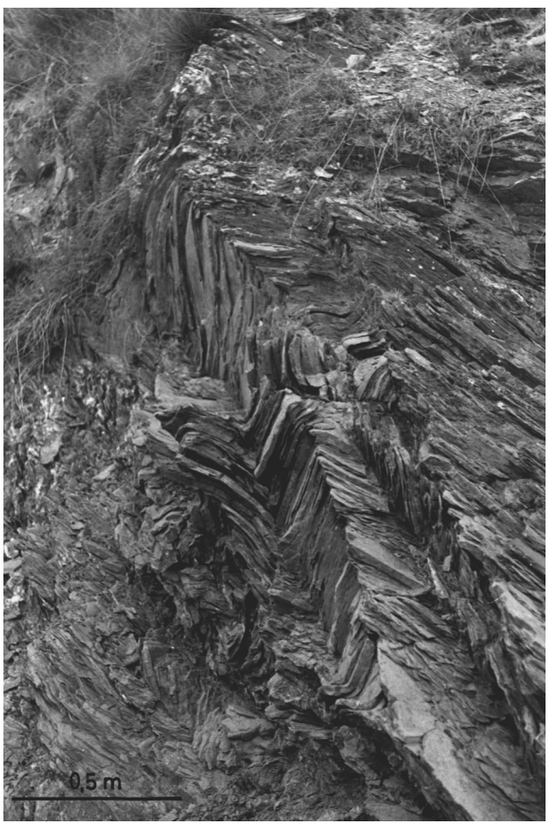

FIGURE 10.19 Kink folds in mica-rich portion of greywackes of the Cantabrian Mountains (northern Spain).

FIGURE 10.20 Ptygmatic folds in the Grenville Supergroup (Ontario, Canada); hammer for scale. Note the wavelength variation as a function of layer thickness.

fold structures that typically occur as tightly folded veins or thin layers of strongly contrasting lithology (and, thus, contrasting competency; Figure 10.20). Most metamorphic regions around the world contain ptygmatic folds, which, unglamorously, resemble intestines.

Doubly plunging folds are structures with hinge lines that laterally change curvature. Along the trend of plunge the folds may die out or even change from antiforms to synforms. The high point of the hinge line in a doubly plunging fold is called the **culmination** and the low point along the same hinge line is called a **depression.** The change in plunge angle is normally less than 50°. When additional folds are present, changes in plunge may result in *en echelon* **folds,** in which a gradually opening fold is replaced by a neighboring, gradually tightening fold of opposite form. Such a geometry occurs on all scales, from hand specimens (Figure 10.21) to the size of mountain ranges (such as the Valley-and-Ridge of the central Appalachians). Note that doubly plunging folds are, by definition, noncylindrical. **Sheath folds**[10] show extreme hinge line curvature, to the extent that hinge line curvature approaches parallelism (change in plunge up to 180°!). What is typically found in outcrop is the elliptical cross section of the nose of the fold (see Figure 12.28); however, such a pattern itself does not necessarily imply a section through a sheath fold. Any doubly plunging fold may give the same outcrop pattern, but only when a highly curved hinge line is visible can

FIGURE 10.21 *En echelon* folds on the scale of centimeters; coin for scale.

[10]They resemble the sheath of a sword; the more imaginative term is *condom fold*.

sheath folds be recognized as such. Sheath folds are produced by taking a mildly doubly plunging fold and "pulling" at its crest, as occurs in zones of high shear strain. We return to the formation and significance of these structures in Chapter 12, which deals with ductile shear zones.

Finally, two additional fold types have been studied extensively in recent years because of their association with hydrocarbon potential in fold-thrust belts, namely, fault-bend folds and fault-propagation folds. Because of their intimate association with thrusting, we further examine their formation and significance in Chapter 18 ("Fold-Thrust Belts"). At this point we merely include them for completeness: **fault-bend folds** are formed as thrust sheets move over irregularities in the thrust plane (such as ramps), whereas **fault-propagation folds** are accommodation structures above the frontal tip of a thrust.

10.6 SUPERPOSED FOLDING

Structural geologists use the term **fold generation** to refer to groups of folds that formed at approximately the same time interval and under similar kinematic conditions. Commonly we find several fold generations in an area, which are labeled by the letter *F* (for *F*old) and a number reflecting the relative order of their formation: F_1 folds form first, followed by F_2 folds, F_3 folds, and so on. Several fold generations may in turn form during an **orogenic phase** (such as the Siluro-Devonian "Acadian" phase in the Appalachians or the Cretaceous-Tertiary "Laramide" phase in the North American Cordillera), which is noted by the letter *D* (for *D*eformation). In any mountain belt several phases may be present, which are labeled D_1, D_2, and so on, each containing one or more generations of folds. For example, the Appalachian Orogeny of the eastern United States contains three main deformation phases (Taconic, Acadian, and Alleghenian). From the onset it is important to realize that neither a deformation phase nor each of the individual fold generations have to be present everywhere along the orogen, nor do they occur everywhere at the same time. On a regional scale *deformation is irregularly distributed and commonly diachronous.* You can imagine that fold generations and deformation phase can rapidly become pretty complex. So we'll stick to two fold generations to examine the principles of superposed folding, which allows us to unravel the sequence (that is, relative timing) of folding.

Generation is a relative time concept and only implies "older than" or "younger than"; you are the younger generation in the eyes of your parents. There are methods to determine the absolute ages of folds, such as dating of minerals that formed during folding, but we will not get into them here. The relative time principle of **superposed folding**[11] is simple: folds of a later generation are superimposed on folds of an earlier generation. The determination of this temporal sequence, however, is not straightforward and requires careful spatial analysis. Superposed folding is a widespread phenomenon that is not restricted to high-grade metamorphic areas. Even in regions below the **greenschist facies** (temperatures below ~300°C), superposed folding is found. It is worthwhile therefore to give attention to this topic, after which we close this section with the concept of fold style that is used to place our findings on fold generations in a regional context.

10.6.1 The Principle of Fold Superposition

Figure 10.22 shows a field photograph of a complex fold geometry that contains two fold generations. How do we know this from looking at the picture and how can we separate F_1 and F_2 folds in this pattern? Fold superposition is simple at its root, but the concept requires the ability to visualize and analyze sometimes very complex three-dimensional geometries. Let us first start with the rule: *a superposed fold must be younger than the structure it folds.* This merely restates the Law of Superposition such that it applies to folding. Unless a fold was present previously, it cannot be modified by a younger fold. How do we determine the criteria by which one obtains this temporal relationship? We begin with an example.

Figure 10.23a shows a sequence of recumbent folds that we will call F_A; the associated axial surface is called S_A. We now superimpose a series of upright folds of approximately the same scale (F_B with axial surface S_B; Figure 10.23c). The superimposition of F_B on F_A produces the interference pattern shown in Figure 10.23b. Elements of both fold generations are preserved; for example, the recumbent nature of F_A is still there, but its limbs are now folded. Similarly, the upright F_B folds remain visible, but they are superposed on a pattern that repeats and inverts bedding (from the recumbent F_A folds). The way to determine the temporal relationship from our interference pattern is to invoke the rule of superposition. Both the bedding

[11]Also called fold superimposition or fold overprinting.

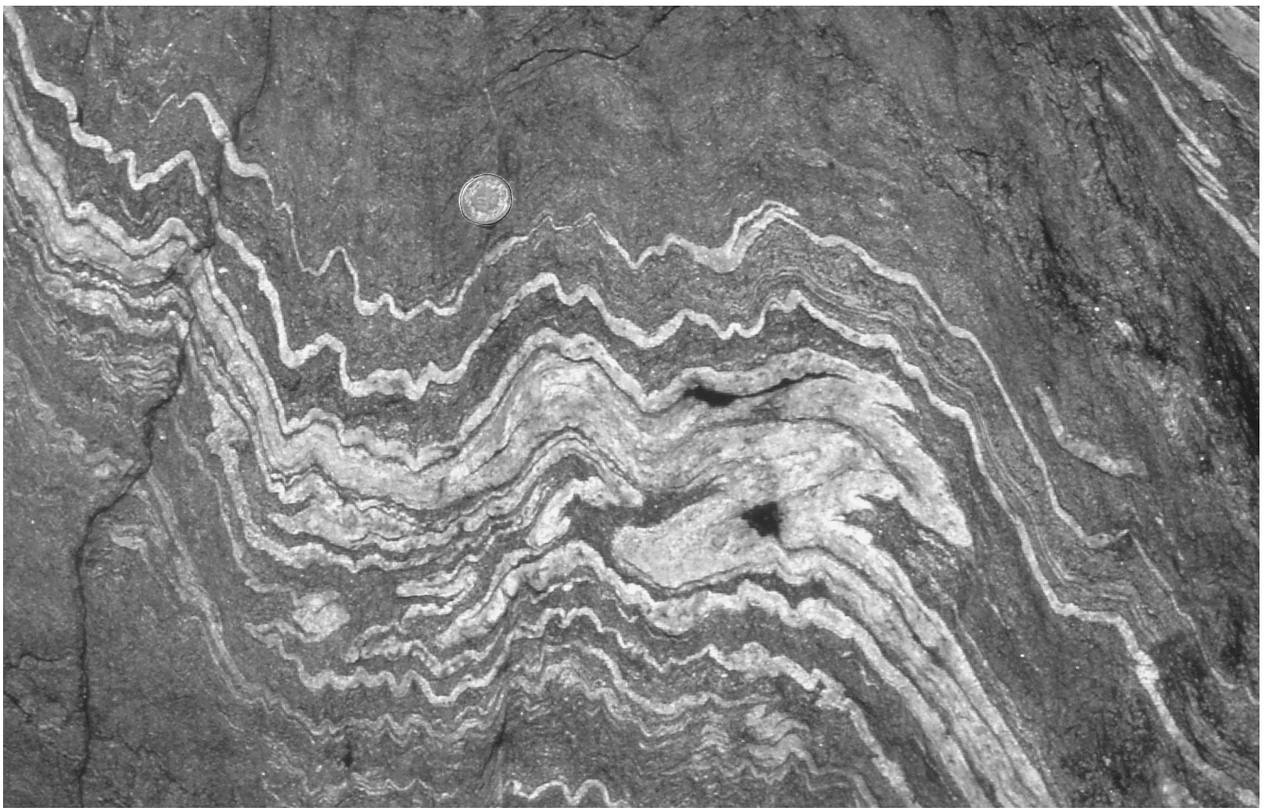

FIGURE 10.22 Fold interference pattern of Type 3 ("refolded fold") geometry.

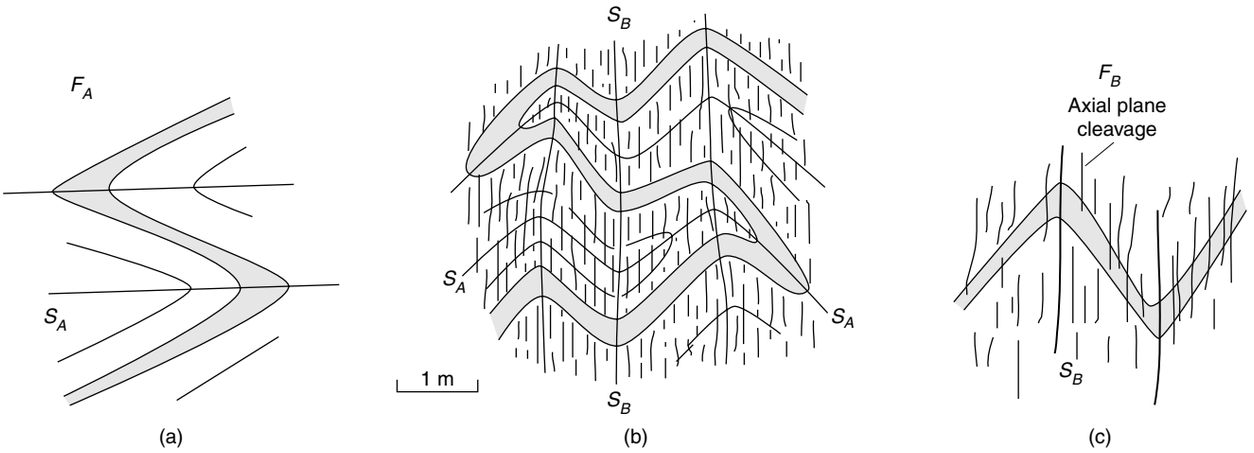

FIGURE 10.23 Dissecting a fold interference pattern. The cross sections show F_A recumbent folds (a) that are overprinted by F_B upright folds (b), producing the fold interference pattern in (c).

and S_A are folded, but S_B is essentially planar. So, bedding and S_A were already present before S_B; consequently, the upright folds must be F_2, which are younger than the recumbent F_1 folds. The axial surfaces may not be always visible in the field (although axial plane foliations are common; Chapter 11), but you can always use an imaginary axial surface to evaluate these complex folding patterns. Now examine this pattern yourself with an analog. Take a piece of paper and fold it in two (our F_1 fold) and orient it into a recumbent orientation. Then fold the paper again to create an upright fold (our F_2 fold) whose hinge parallels the hinge of the recumbent fold. *Voilà,* you get the pattern of Figure 10.23b. If you are comfortable with

this example, we will proceed with the four basic fold interference patterns.

10.6.2 Fold Interference Patterns

Four basic patterns are recognized from the superimposition of upright F_2 folds on F_1 folds of variable orientation (Figure 10.24). Looking at these **fold interference types** you will notice that we produced Type 3 using the piece of folded paper above. Types 0 and 2 can equally well be examined by folding a piece of paper, but Type 1 requires additional crumpling. Instead of describing these patterns in confusing words, look at Figure 10.24 and reproduce the geometries with a piece of paper and your hands. An approach that may offer further insight is to make fold

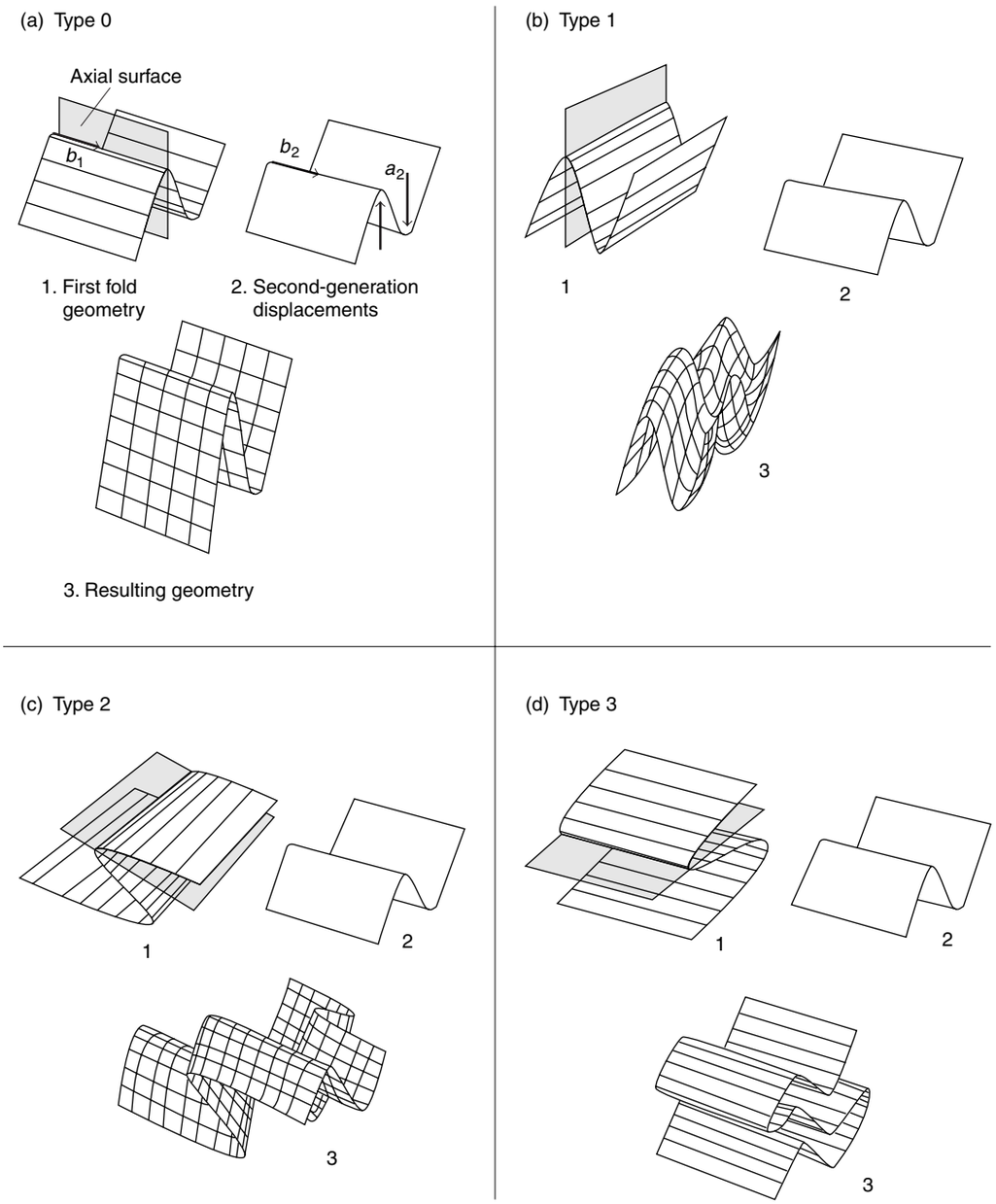

FIGURE 10.24 The four basic patterns arising from fold superposition. The analysis assumes that F_2 shear folds (a_2 is the relative shear direction and b_2 is the hinge line) are superimposed on a preexisting F_1 fold of variable orientation. Shear folds are modeled by moving a deck of cards. The shaded surface is the S_1 axial surface.

interference patterns using a few thin layers of colored modeling clay, which can then be cut with a knife to see the effect of intersecting surfaces. Open a refreshing drink and start your experimentation. . . .

Welcome back from spending time with clay, paper, and Figure 10.24. We now turn to some important properties of the various fold interference types. Type 0 is a special condition, because the hinge lines and the axial surfaces of both fold generations are parallel. As a consequence, F_1 is merely tightened by the superimposition of F_2. You realize that, practically, Type 0 cannot be recognized in the field as an interference type by geometry alone (that's why we use the number 0). Type 1 is also called a "dome-and-basin" structure and resembles an egg carton. Both the axial surfaces and the hinge lines of the two generations are perpendicular, producing this characteristic geometry (Figure 10.24a). Type 2 is perhaps the most difficult geometry to visualize, but folding a piece of paper helps enormously. In outcrop, we often see a section through this geometry that resembles a "mushroom" pattern (Figure 10.24b). Note that this outcrop pattern is only generated in the horizontal surface that intersects Type 2; if we take another cut, say vertical, the outcrop pattern is quite different. Finally, Type 3 (Fig-ure 10.24c) is sometimes referred to as the "refolded fold" pattern, which is a misnomer because all four types are refolded folds. We just present the name so that you have heard it, and because very few people are otherwise able to remember the corresponding numbers of the types. We recommend that you use the descriptive terms "dome-and-basin," "mushroom," and "refolded-fold," however flawed, instead of the abstract Type 1, Type 2, and Type 3, respectively.

Interference patterns are a function of the spatial relationship between hinge lines and axial surfaces of the fold generations, as well as the sectional surface in which we view the resulting patterns. Thus, the analysis of fold superposition is a three-dimensional problem. The four types that are shown in Figure 10.24 are only end-member configurations in an infinite array of possibilities. Figure 10.25 is a summary diagram that shows patterns from varying the spatial relationships between fold generations, as well as the observation surface (or, the outcrop). Even more so than before, understanding these patterns requires self-study. Ultimately, interference patterns reward you with complete information on the sequence and orientation of fold generations. So, again take your time.

The fold interference patterns we have analyzed are produced when fold generations of similar scale are superimposed. If the scales are very different there may be no interference pattern visible on the outcrop scale, and only through regional structural analysis does the large-scale structure appear. After some field work it is therefore not uncommon to find one or more additional fold generations that only show on the map scale. A reexamination of some puzzling field notes and outcrop sketches may all of a sudden be explained by recognizing this missing fold generation.

The presence of multiple fold generations has major implications for the interpretation of the deformation history of your area. First, it implies that the kinematic conditions have changed to produce a fold generation with different orientation than before (except Type 0); so the deformation regime must somehow have changed. Secondly, folds of the first generation will have variable orientations depending on where they are measured in the fold superposition pattern. Orientation, therefore, is *not* a characteristic of fold generations in multiply deformed areas and should be used carefully as a mapping tool (see below). That leaves a final question: How do we recognize folds of a certain generation in the absence of interference patterns at each and every locality in our area? For this we turn to the powerful concept of fold style.

10.6.3 Fold Style

When we encounter a number of folds in our field area, the logical question of their significance arises. Are they part of the same generation or do they represent several generations? Say that, at one locality in our area, we are actually able to determine a sequence of F_1 and F_2 folds, so we know that there are at least two generations. From our experience with superposed folding, we are also aware that only F_2 folds have an orientation that may persist over any distance, and that the orientation of F_1 folds depends entirely on their position in the fold interference pattern (we measure their orientation nonetheless because the distribution should "fit" the pattern). We now are at an outcrop where we only find one fold, which is not in the exact same orientation as either F_1 or F_2 in the previous outcrop. Nonetheless we wish to predict to which generation it belongs, and for that we use characteristics for each fold generation that are grouped under the term **fold style.** The fold style characteristics are listed in Table 10.4.

The four elements of Table 10.4, parallel/similar, interlimb angle, cylindrical/noncylindrical, and foliations/lineations, are used to describe the style of a fold. The first three have been discussed in detail and need no further clarification. Foliations and lineations will have more meaning after you read Chapter 11, but this fourth characteristic is included here because of its discriminatory ability. For example, an axial plane

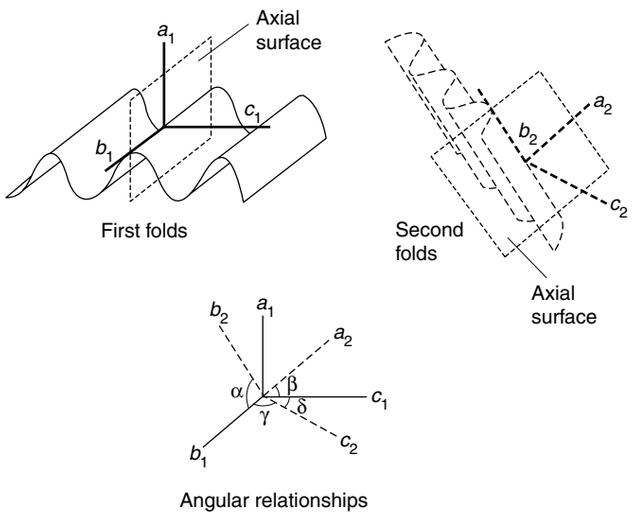

(a)

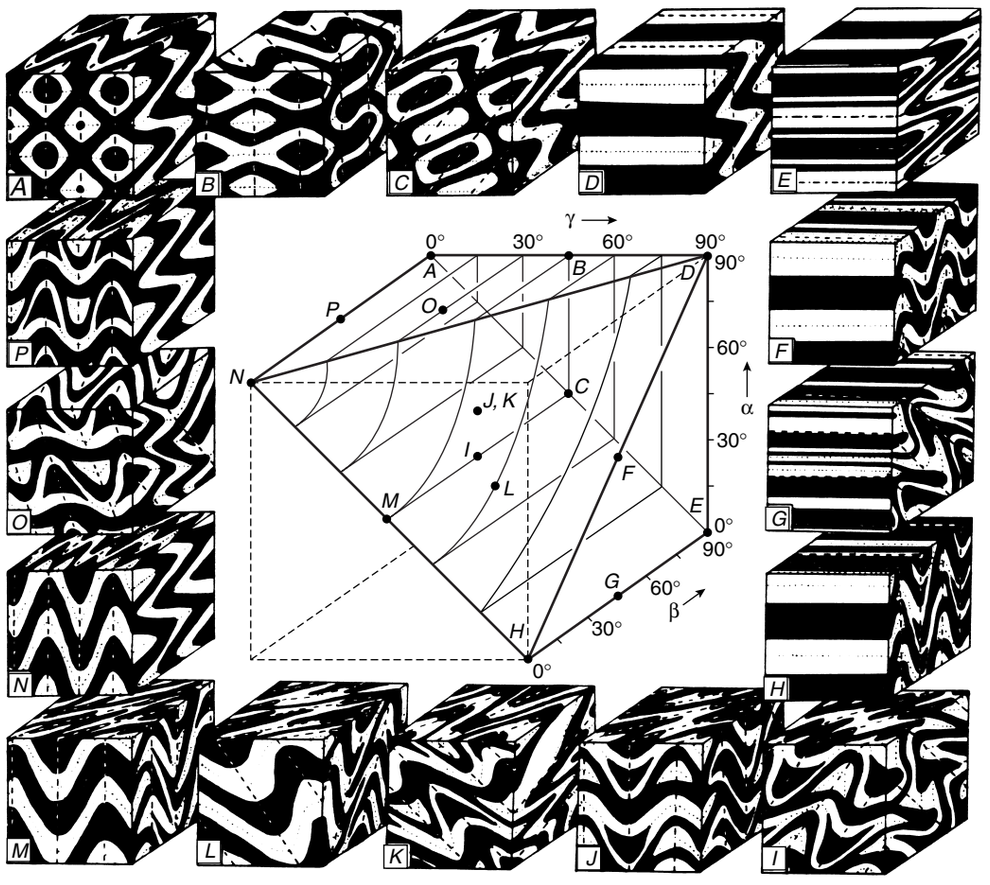

(b)

FIGURE 10.25 Geometric axes describing the orientation of fold generations F_1 and F_2 (a), and corresponding interference patterns (b). In all patterns, the layering was initially parallel to the front face of the cube. F_1 resembles case *D;* F_2 is similar to the folding in case *D,* but with different orientations. Axial surface S_1 is shown with dotted lines and axial surface S_2 with dashed lines.

TABLE 10.4	THE CHARACTERISTIC ELEMENTS OF FOLD STYLE

- In profile plane, is the fold classified as parallel or similar (or a further refinement)?
- What is the interlimb angle in profile?
- In three dimensions, is the fold cylindrical or noncylindrical?
- Is there an associated axial plane foliation and/or lineation present, and of what type are they?

Note that orientation and symmetry are not style criteria.

crenulation cleavage may be a characteristic of F_2 folds, and the presence of a mineral lineation may reflect special metamorphic conditions that only occurred during the first fold generation. Notably absent in our list are fold orientation and fold symmetry, which are not style criteria. Discriminating a fold generation on its orientation may only work for the last fold generation; the older ones most likely have become variably oriented. Secondly, we already learned that fold symmetry may change within a single-generation, large fold (Figure 10.16). So, just like orientation, symmetry is not a style criterion.

10.6.4 A Few Philosophical Points

We close the section on superposed folding with a few considerations. You will often find that it is not possible in any single outcrop to determine the complete sequence of fold generations, because discriminatory interference patterns may not be exposed, or one or more generations may not be visible at all. However, by combining information from several outcrops as well as using fold style you should eventually be able to obtain a reasonable fold sequence. As you map, you should continue to test this hypothesis, and after a thorough job the foundation on which you base the folding sequence will be firm. Only then will the time have come to place your findings in a regional kinematic picture. For example, you may find that the first generation of folds is recumbent, which we quite commonly associate with nappe style, and that the second fold generation is upright, reflecting folding of the thrust sequence. Maybe yet a third fold generation reflects a very different shortening direction, possibly related to a different orogenic phase. We may also find small kink folds in well-foliated rocks that complete the deformation sequence. Although the possibilities seem limitless, reasonable interpretations are not.

There is sometimes a tendency to recognize too many fold generations by structural geologists. In the end, the number of fold generations should be based *only* on interference patterns, on either local or regional scales. Practically, in any one outcrop you may be able to see two or three fold generations, and regionally perhaps a couple more. Remember that structural analysis is not helped by proposing an unnecessarily long and complex sequence of fold generations, because each generation must reflect a corresponding deformation regime. One can reasonably expect only so many different tectonic patterns. With these musings and a closing field example of a Type 1 fold interference pattern (Figure 10.26), we leave the descriptive part of folds and field analysis to turn our attention to the mechanics of folding.

10.7 THE MECHANICS OF FOLDING

Why does folding occur? After spending so much time on the description of folds, this is a question whose time has come. Well, if you ever saw a car collision you do not need to be reminded that forces can cause folding.[12] Indeed, forces applied to rocks cause folding, but we will see that forces alone are not sufficient to form folds. Consider a block of clay that is reshaped by external forces (from your hands). The block will change form, but in doing so the internal structure does not show any folds (Figure 10.27a). After we add irregularly shaped layers of different color but with the same material properties to the block, we get folds when the irregularities are amplified (Figure 10.27b). If we add straight, thin sheets of rubber to our clay block and a force is applied, folds also appear (Figure 10.27c). These experiments provide us with a fundamental subdivision of folding based on the mechanical role of layers: passive folding and active folding.

10.7.1 Passive Folding and Active Folding

During **passive folding** the layering of a material has no mechanical significance. In the color-banded clay block, folds are formed by the amplification of small

[12]This recurring analogy does not reflect the authors' personal experiences.

FIGURE 10.26 Fold interference pattern of Type 1 ("dome-and-basin") geometry; compass for scale.

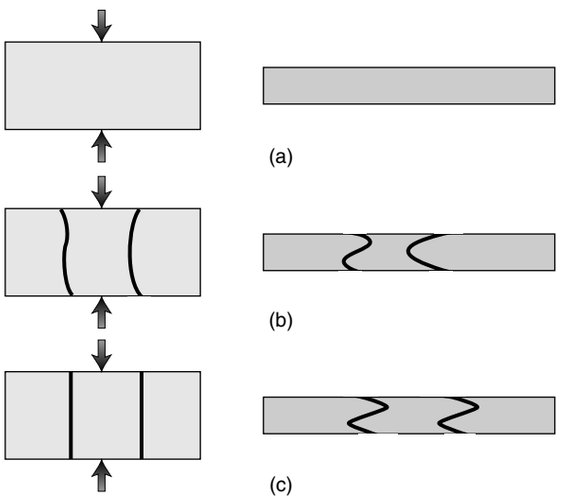

FIGURE 10.27 Compression of a clay block of uniform color (a), with irregularly shaped layers of different colors (b), or with uniform colored layers separated by thin sheets of rubber (c).

perturbations in the bands, but the strain pattern in the block is unaffected by the presence of these layers. Squeezing multicolor toothpaste on a counter top is a fresh and minty experiment where complex folding patterns are visible only because of the color contrast; if you do the same experiment with single-color toothpaste you will not see folds, even though the internal structure of the two blobs is similar. We find such toothpaste-like behavior in nature where rocks have little or no competency contrast between layers. Elevated temperatures can produce the right conditions for passive folding and it is common to find toothpaste-like structures in deformed metamorphic rocks. Rocks that were deformed at or near their melting temperature (that is, a high homologous temperature, $T_h = T/T_m$) are called **migmatites,** which often contain wonderfully complex fold structures (see Figure 2.22). Similarly, passive folding occurs in glaciers that deform close to their melting temperature. Passive folds are the ampli-

fication of natural irregularities in the layers, or are a consequence of differential flow in a volume of rock. But don't think that passive folds have to be chaotic in appearance because of this. Sheath folds in a shear zone are another natural example of passive folding and typically show very consistent orientation and style.

During **active folding,** also called **flexural folding,** the layering has mechanical significance. This means that the presence of layers with different competency directly affects the strain pattern in the deforming body and that there is contrasting behavior between layers. There are two dynamic conditions that we distinguish for active folding: bending and buckling. In *bending,* the applied force is oriented at an oblique angle to the layering (Figure 10.28a). In nature this may occur during basin formation or loading of a lithospheric plate (also called flexural loading), or during the development of monoclines over fault blocks. In *buckling,* the force is oriented parallel to the mechanical anisotropy (Figure 10.28b), the most common situation for folding.

Let's see what happens in a series of analog experiments of active folding, in this case buckling (Figure 10.29). We surround a band of rubber with foam in a plastic box that is open at one end, at which we place a plunger. As we push on the plunger, the band of rubber forms a series of folds. The surrounding foam (the "matrix") accommodates the shape of the rubber band by filling the gaps that would otherwise be present. We repeat the experiment with a thinner band of rubber and the same foam. Now we produce several more folds and the weaker foam again accommodates this new pattern. So, in spite of applying the same force and producing the same bulk shortening strain, the folding patterns are different as a function of the thickness of the rubber band. In other words, the rubber band introduces a **mechanical anisotropy.**

10.7.2 Buckle Folds

We return to the above rubber band–foam experiments, where we saw that the thickness of the band somehow affects the fold shape, to explore some systematic properties of buckle folds. The applied force (and thus stress), the bulk strain (the distance the plunger moves into our box), the strain rate (the speed at which the plunger moves), and the ambient conditions (room temperature and pressure) are assumed to be the same in all experiments; only thickness, *t,* of the layer varies. We notice that with increasing thickness the wavelength and arc length become larger. Secondly, if we use bands of equal thickness but with different

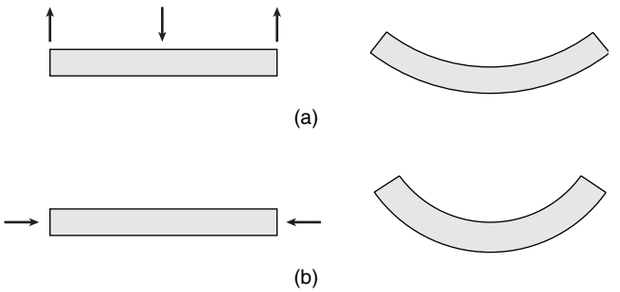

FIGURE 10.28 Bending (a) and buckling (b) of a layer.

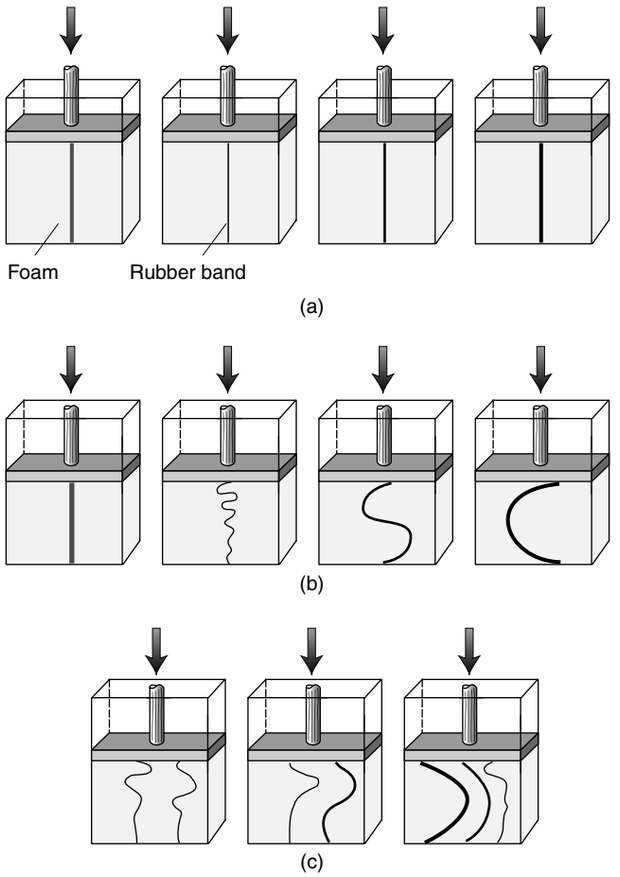

FIGURE 10.29 Line drawings of deformation experiments with transparent boxes containing foam, and rubber bands. In (a), four starting settings are shown that contain, from left to right, foam only (with marker line added), a thin, a medium, and a thick rubber band. When applying the same displacement, shown in (b), the setups respond differently. The foam-only box shows thickening of the marker line, but no folding. The boxes with rubber bands show folds with arc lengths varying as a function of thickness of each band. When using more than one band (c), the behavior depends on the combination of bands and their thicknesses, with the effect of the thicker bands being dominant.

stiffness, we find that arc length of the stiffer layer is larger than that of the weaker layer. So, we find that both thickness and the parameter "stiffness" increase the wavelength. In nature, we are not really dealing with elastic layers. Folds are permanent strain features, so it is more useful to consider this problem in terms of viscous behavior or even more complex rheologic models (such as elastico-viscous or nonlinear viscosity; Chapter 5). For our current purposes we assume simple, Newtonian (linear) viscous behavior.

Using Newtonian viscosity, the theoretical arc length–thickness relationship for a layer with viscosity η_L surrounded by a matrix with viscosity η_M is:

$$L = 2\pi t\,(\eta_L/6\eta_M)^{1/3} \qquad \text{Eq. 10.1}$$

This equation, which is known as the **Biot-Ramberg equation,**[13] tells us that arc length (L) is directly proportional to thickness and to the cube root of the viscosity ratio. Therefore, if we know the arc length/thickness ratio of a layer, we can obtain the viscosity ratio. Reorganizing Equation 10.1, we get

$$\eta_L/\eta_M = 0.024\,(L/t)^3 \qquad \text{Eq. 10.2}$$

This formulation states that the viscosity ratio is proportional to the cube of the L/t ratio. The measurements of folded sandstone layers in sedimentary rocks, shown in Figure 10.30, give a viscosity ratio of about 475. We intentionally say "about," because Figure 10.30 is a log–log plot, meaning that a small change in L/t ratio will result in a large change in viscosity ratio. Note that the same analysis for our box experiments above produces a viscosity contrast on the order of 1000, meaning that these experiments are a reasonable approximation of low-grade sandstone deformation.

There is an important consequence when the viscosity ratio of layer and matrix is small (say, <<100). Again we return to our box experiments. This time we place only foam in our plastic box. On the foam we draw a vertical line with a marker pen (Figure 10.29) to represent a layer with a small viscosity ratio (in this case, of course, $\eta_L/\eta_M = 1$). As we compress the foam we do not get any folds, but we find that the layer thickens. So, low viscosity contrasts result in a pronounced component of strain-induced *layer thickening.* We simplify this effect in our analysis by inferring that a component of layer thickening occurs before folding instabilities arise. Recalling the effect of layer thickness on L (Equation 10.1), we therefore include a strain component in Equation 10.1:

$$L = 2\pi t\left[\frac{\eta_L(R_S - 1)}{6\eta_M \cdot 2{R_S}^2}\right]^{1/3} \qquad \text{Eq. 10.3}$$

where R_S is the strain ratio X/Z. This **modified Biot-Ramberg equation**[14] gives a reasonable prediction for the shape of natural folds in rocks with low viscosity contrast, such as one finds in metamorphic regions.

The respective roles of viscosity contrast and layer thickening during shortening are also well illustrated in numerical models of folding. The advantage of mathematical models is their ability to vary parameters with ease. Figure 10.31 shows the results of one series of computer simulations of single-layer folding using a finite-element method. As we already saw in the physical experiment, with decreasing viscosity ratio, the arc length becomes less and the layer increasingly thickens. Another advantage of computer modeling is that we can also track the strain field in our system. Note, for example, the strain pattern in and immediately surrounding the folded layer, which is shown by the

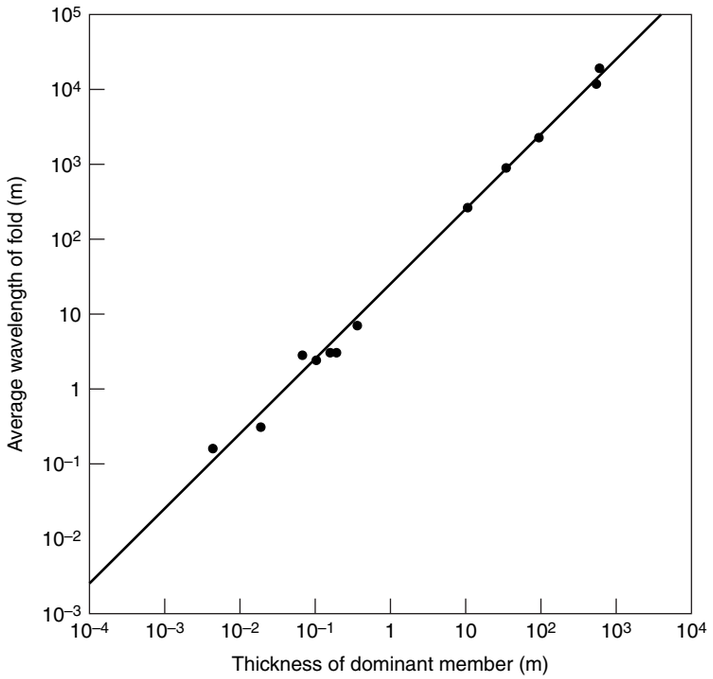

FIGURE 10.30 Log–log plot of wavelength versus layer thickness in folded sandstone layers.

[13]Biot and Ramberg independently carried out this analysis in the early 1960s.

[14]Also known as the *Sherwin-Chapple equation,* after its authors.

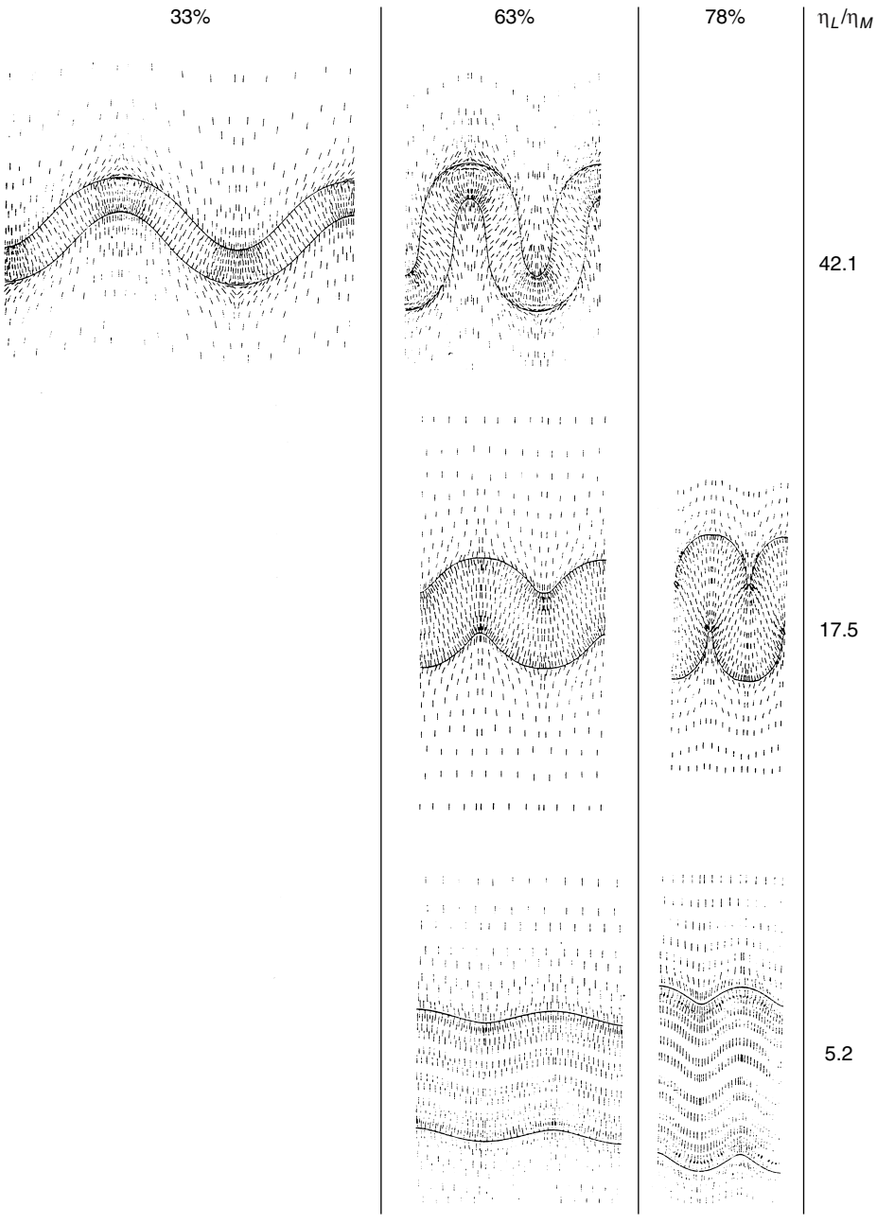

FIGURE 10.31 Finite-element modeling of single-layer buckling for various viscosity contrasts between layer (η_L) and matrix (η_M), and shortening strains (%). The short marks represent the orientation of the long axis of the strain ellipse in profile plane.

orientation of the *x*-axis in Figure 10.31. The strain pattern is increasingly homogeneous with decreasing viscosity contrast. Indeed, no viscosity contrast ($\eta_L/\eta_M = 1$) reflects the situation in which there is no more mechanical significance to the layer (see the foam-only box experiment in Figure 10.29).

These analyses of folding are entirely based on Newtonian-viscous behavior of both the layer and the matrix. However, it is likely that folding under elevated conditions of pressure and temperature involves nonlinear rheologies, in which the viscosity is stress dependent (Chapter 5). Without going into any details, we only mention that appropriate nonlinear rheologies result in lower values of L/t as well as small to negligible components of layer-parallel shortening. Natural folds in metamorphic terrains typically have low L/t ratios ($L/t < 10$), suggesting that nonlinear viscous rheology, and therefore crystal-plastic processes, are indeed important during folding under these conditions.

10.7.3 Folded Multilayers

Our discussion so far has focused on folding of a single layer in a weaker matrix. While this situation occurs in nature, it is not representative. What happens when several layers are present? Again we turn to our simple experimental setup (Figure 10.29), but now use two rubber bands of equal thickness to see what folds develop. Can you explain why the results differ from those of our previous single-layer experiments? The wavelength in the multilayer experiment is greater and the two layers seem to act as a thicker single layer. In another experiment we combine a thick and a thin layer (Figure 10.29). In this case, the thin layer does not at all give the fold shape predicted from single-layer theory, while the thick layer behaves pretty much the same as predicted from the single-layer experiment. In fact, the thin layer mimics the shape of the thick layer, indicating that its behavior is dominated by that of the thick layer. We can try many other combinations, which all show that the behavior of a multilayer system is sensitive to the interaction between layers. The previous Biot-Ramberg buckling theory, therefore, only applies when layers in natural rocks are sufficiently far removed from one another to avoid interaction. We can theoretically determine the region over which the effect of a buckled layer in a weaker matrix dies off to negligible values. This is known as the **contact strain zone (CSZ).** The width of this contact strain zone ($2d_{CSZ}$, where d_{CSZ} is the distance measured from the midpoint of the buckled layer) is a function of the arc length:

$$d_{CSZ} = 2/\pi L \qquad \text{Eq. 10.4}$$

Practically this means that the width of the CSZ is slightly greater than the arc length of a fold, which seems supported by field observations on natural folds.

Interacting layers require a relatively simple extension of the theory of folding, if we assume a stack consisting of several superposed thin layers that are free to move relative to one another (that is, no coupling). The corresponding equation for this multilayer case is

$$L_a = 2\pi t\,(N\eta_L/6\eta_M)^{1/3} \qquad \text{Eq. 10.5}$$

where L_a is the arc length of the multilayer, N is the number of layers, and the space between the layers is infinitely small. Note that this is not the same as the equation for a single layer with the same thickness ($N \cdot t$). If we calculate the ratio of the arc length of a system with N superposed multilayers (L_m) and a system with a single layer of thickness Nt (L_s) by dividing Equation 10.1 (with $t = Nt$) and Equation 10.5, we get

$$L_s/L_m = N^{2/3} \qquad \text{Eq. 10.6}$$

This shows that the arc length of N multilayers of thickness t is less than that of a single layer with thickness Nt. This scenario is certainly not applicable to all geologic conditions. Commonly we find that layers of one viscosity alternate with layers of another viscosity. For example, a turbidite sequence contains alternating layers of sandstone and shale. In this case the analysis is considerably more complex and, because increasingly restrictive assumptions have to be made (including the spacing between layers), we stop here. The main point is that multilayers behave much like a thick single layer, but the resulting arc length in a multilayer system will be less than that of a single layer.

10.8 KINEMATIC MODELS OF FOLDING

The distinction we made earlier between active and passive folds describes the mechanical role of layers under an imposed stress, but this says little about the inner workings of the folded layer and the associated strain pattern. To this end, we differentiate between three fundamental models, flexural folding, neutral-surface folding, and shear folding, as well as modification of folds by superimposed strain; each of these have distinct properties and characteristics. These models are compared with natural examples in the final section.

10.8.1 Flexural Slip/Flow Folding

Take a phone book or a deck of playing cards, and bend it into a fold.[15] The ability to produce the fold is achieved by slip on the surfaces of the cards relative to one another, without appreciable distortion within the surface of any individual card (they remain of the same size). If we place small marker circles on the top surface as well as on the sides of the card stack for use as a strain gauge, we see that strain only accumulates in surfaces that are at an angle to the individual cards

[15]Computer punch cards are well suited, but remain only in the possession of old structural geology instructors.

(that is, the sides) when we fold the deck. The circles become ellipses in the profile plane (Figure 10.32) and on the other side of the folded deck parallel to the hinge line. Within the plane of each card, however, there is no strain, as seen from the fact that the circles on the top card in the deck remain circles. Folds that form from slip between layers are called **flexural slip folds.** The amount of slip between the layers increases away from the hinge zone and reaches a maximum at the inflection point. Moreover, the amount of slip is proportional to limb dip: slip increases with increasing dip. The card deck analogy highlights three important characteristics of flexural slip folding. First, at each point in the profile plane the strain ratio and orientation differ. Second, in three dimensions the strain state of the fold is plane strain ($X > Y = 1 > Z$), with the orientation of the intermediate strain axis (Y) parallel to the hinge line. Third, a geometric consequence of the flexural slip model is that the fold is cylindrical and parallel (Class 1B); the bed thickness in flexural slip folds does not change. The geometric consequences of flexural slip folding are not diagnostic of the model, because they also occur in other models (see neutral-surface folding to follow). The strain pattern, however, is. Chevron folds (Figure 10.8) and kink folds (Figure 10.19) are examples of flexural slip folding in natural rocks that form because of a strong layer anisotropy. Slip that occurs on individual grains within a layer, without the presence of visible slip surfaces, we call *flexural flow folding.*[16] Although they differ in a few details, the geometric and kinematic consequences of both flexural slip and flexural flow folding are alike.

A diagnostic feature of flexural slip folding that can be used in field analysis is that any original angular relationship in the slip surface before folding (say, flute casts in the bedding surfaces of turbidites) will maintain this angular relationship across the fold, because there is no strain on the top and bottom of the folded surface. Consequently, a lineation at an angle to the hinge line will distribute as a cone around the hinge line with that angle (a small-circle pattern in spherical projection).

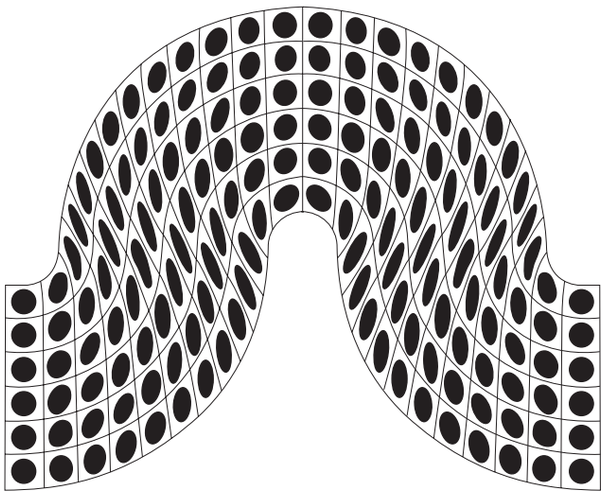

FIGURE 10.32 The characteristic strain pattern of flexural folding in the fold profile plane (the plane perpendicular to the hinge line).

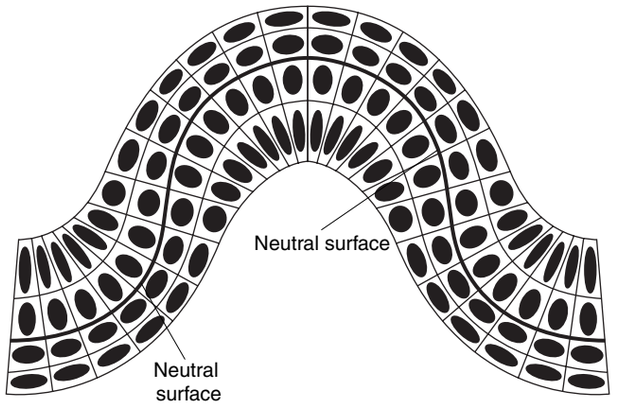

FIGURE 10.33 The strain pattern of neutral-surface folding in the fold profile plane.

10.8.2 Neutral-Surface Folding

When we bend a layer of clay or a metal bar we obtain a fold geometry that seems identical to one produced by flexural folding, but with a distinctly different strain pattern. This is illustrated by tracking the distortion of circles drawn on the sides of the undeformed layer (Figure 10.33). On all three surfaces we find that circles have become ellipses, including the folded top and bottom surface. On the top folded surface, the long axis of each ellipse is perpendicular to the hinge line, but on the bottom the long axis is parallel to the hinge line. In the profile plane the long axis is parallel or perpendicular to the top and bottom surfaces of the folded layer, depending on where we are in that plane (Figure 10.33). There must, therefore, be a surface in the fold where there is no strain. This zero-strain surface gives the model its name, **neutral-surface fold.** Trying to mimic this behavior with the deck of cards used

[16]Flexural flow folding has also been used to describe the migration of material from the limbs to the hinge area of folds, but we do not adopt this usage here.

earlier will require some muscle power, because the cards in the outer arc need to stretch while those in the inner arc are compressed.

The fold shape from neutral-surface folding is parallel and cylindrical, with the intermediate bulk strain axis parallel to the fold axis. These geometric characteristics and plane strain conditions also hold for flexural slip folding, so they are not diagnostic for either model; their strain patterns, however, are. Because strain accumulates in the folded surfaces during neutral-surface folding, the orientation of any feature on these surfaces changes with position in the fold. In the outer arc an initial angle with the hinge line increases, while in the inner arc this angle decreases. So, the angle of flute marks with the hinge line on the top surface of the folded layer increases, while on the bottom surface this angle decreases. In both cases the orientations in any individual surface describe neither a cone nor a plane (or small circle and great circle in spherical projection, respectively). Only in the neutral surface is the angle unchanged and does the linear feature describe a cone around the hinge line. It is not easy to use this criterion as a field tool unless one measures lineations from individual top and bottom layers in a fold. The strain pattern in the profile plane, however, is more characteristic, and is (cumbersomely) called **tangential longitudinal strain.** Note that the position of the neutral surface is not restricted to the middle of the fold, nor does it necessarily occur at the same relative position across the fold. In extreme cases the neutral surface may coincide with the outer arc, in which case the long axis of each strain ellipse in the profile plane is perpendicular to the folded surface. Is it possible to have the neutral surface at the inner arc? Answer this question to test your understanding of neutral-surface folding before moving on to the third and final folding model.

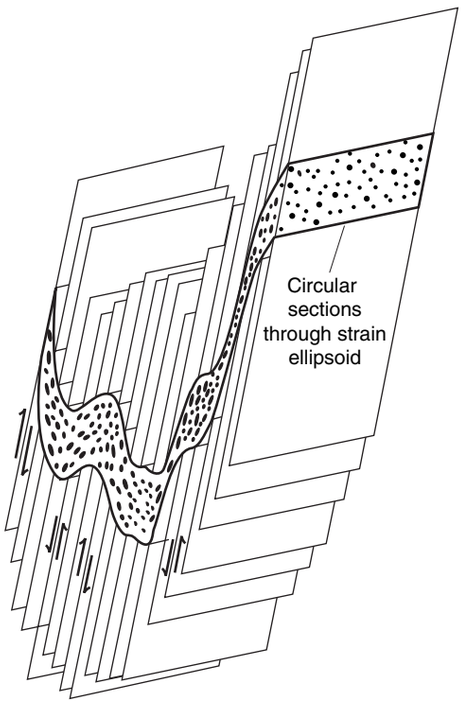

FIGURE 10.34 The strain pattern of shear folding.

10.8.3 Shear Folding

To represent shear folding, we again turn to a deck of cards, but now we draw a layer on the sides of the deck. When we differentially move the cards relative to one another we produce a fold by a mechanism called **shear folding** (Figure 10.34). The fold shape varies with the amount and sense of displacement between individual cards and the layer has no mechanical significance; that is, shear folds are passive features. While slip occurs on individual cards, the slip surface and the slip vector are not parallel to the folded surface, as they are with flexural folding. Circles drawn on the deck before we shear the cards show that there is no strain in the surface of individual cards, but there is strain in the other surfaces. The overall strain state is plane strain, but the hinge line is not by definition perpendicular to the displacement vector, nor parallel to the intermediate (Y) strain axis. Most notably, the folds we produce have a distinct shape, because the trace of the layer on each card remains equal in length after shearing. As a consequence, we produce similar folds (Class 2). It is about time that we produced this class of folds, which are common in the field, while our models so far only generated parallel folds, which are not. Much of the charm of shear folding lies in the ability to form similar folds, which are only formed by the other two mechanisms after additional modification (see Section 10.8.4).

In nature, there are no playing cards slipping past one another. Axial plane cleavage (which is discussed in Chapter 11) may act as shear planes,[17] but rocks mostly flow as a continuum. Shear folds can be formed in regions where the flow field is heterogeneous, such as in glaciers (see fold geometry in Figure 10.1). In shear zones, relatively narrow regions with high shear strains (Chapter 12), a mylonitic foliation is common and may act as a shear plane for shear folding. In fact, sheath folds are a spectacular example of the development of such passive folds.

[17]Axial plane cleavage cannot exactly parallel the finite XY principal plane of strain, as this is not a shear plane.

10.8.4 Fold Shape Modification

The appeal of shear folding is the formation of similar (Class 2) folds, whereas both flexural folding and neutral-surface folding produce parallel (Class 1B) folds. What happens in the latter scenarios when we allow modification of the fold shape? Experiments and geometric arguments place a limit on the degree of strain that can be accumulated by fold tightening in parallel folds. You may have noticed this when folding the card deck, where the inner arc region increasingly experiences space problems as the fold tightens (Figure 10.11a). Material that occupies the inner arc region may be able to accommodate this space crunch, much like the foam does in our box experiments. However, as the fold tightens, the later strain increments will increasingly affect the entire fold structure (limbs and hinge equally), resulting in **superimposed homogeneous strain.** This strain component has a pronounced effect on the fold shape.

Figure 10.35 shows the effect of superimposed homogeneous strains (constant volume, plain strain) with 20% shortening ($X/Z = 1.6$) and 60% shortening ($X/Z = 6.3$) on shape and corresponding strain distributions in a flexural fold and a neutral-surface fold. You see that initially parallel folds change shape by thinning of the limbs relative to the hinge area, resulting in a geometry that approaches similar folds (Class 1C). Perfectly similar (Class 2) folds are only achieved at an infinite X/Z ratio, which is obviously unrealistic. A reminder on strain superimposition. In Chapter 4 you learned that strain is a second-rank tensor, and that tensors are not commutative; that is, $\mathbf{a}_{ij} \cdot \mathbf{b}_{ij} \neq \mathbf{b}_{ij} \cdot \mathbf{a}_{ij}$. This implies that we get different finite strains when we reverse the sequence of parallel folding and homogeneous strain, or simultaneously add homogeneous strain during folding. The implications of these scenarios are explored in more advanced texts, as they require tensor calculations.

In all models we fail to produce Class 3 folds, which pose the final challenge. One likely scenario for the formation of Class 3 folds lies in the interaction between layers of different competency in a multilayered system. Consider a sequence of shale and sandstone layers (Figure 10.36). As we shorten the sequence, the strong (competent) sandstone layers form Class 1B to 1C folds (as outlined above). The weaker (less competent) intervening shale layers accommodate the shape of the folded sandstone layers when they are in the contact strain zone. This means that folds of Class 3 will be formed in intervening shale when the sandstone layers are closely spaced, and folds of Class 1C to 2 when the sandstone layers are farther apart.

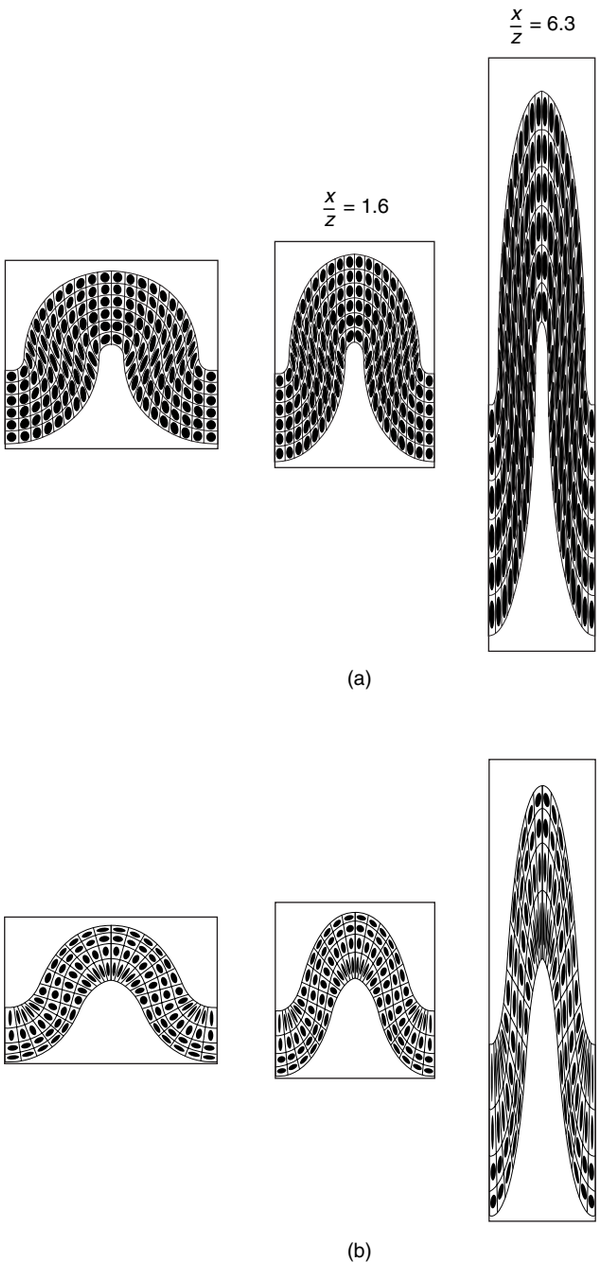

FIGURE 10.35 The effect of superimposed homogeneous strain on (a) a flexural and (b) a neutral-surface fold. Constant volume, plane strain with $X/Z = 1.6$ (20% shortening), and $X/Z = 6.3$ (60% shortening) are shown.

10.8.5 A Natural Example

How well does all this theory apply to nature? To answer this, we look at an example of a parallel fold in a limestone-pebble conglomerate. Strain values that were measured from pebbles across the folded layer give an estimate of the overall strain pattern (Figure 10.37a). When comparing this pattern with those predicted for flexural folding (Figure 10.37c) and

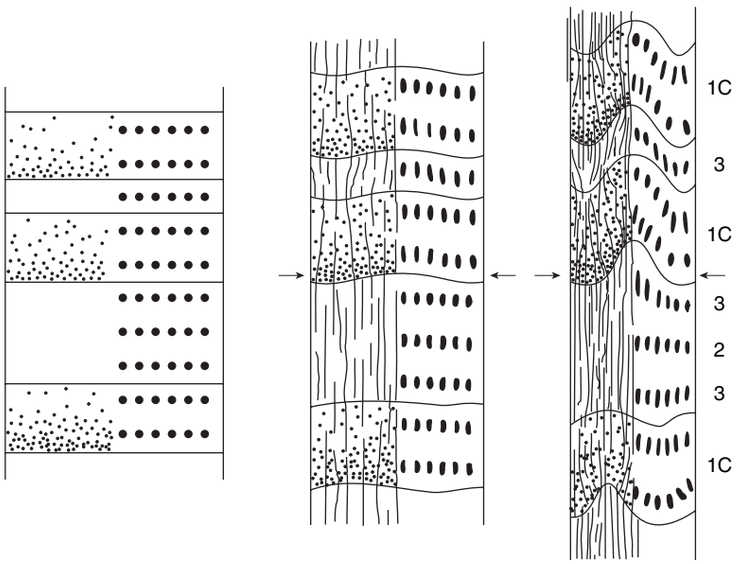

FIGURE 10.36 Folding of a multilayer consisting of sandstone (stippled) and shale layers. The incompetent shale layers accommodate the strong sandstone layers. This results in Class 3 and Class 2 folds in shale when the sandstone layers are closely and more widely spaced, respectively. The sandstone layer forms Class 1 folds.

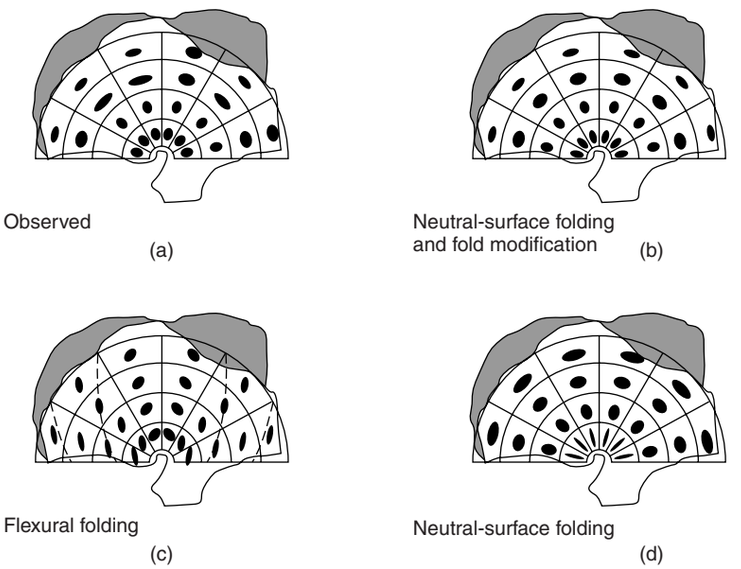

FIGURE 10.37 Strain pattern in a natural fold of limestone-pebble conglomerate (a). This pattern more closely resembles the strain predicted in neutral-surface folding (d) than in flexural folding (c). With further modification, which consists of initial compaction and material transport away from the inner arc region, a strain pattern much like that observed in the natural sample can be produced (b).

neutral-surface folding (Figure 10.37d), we see that the natural pattern most resembles that predicted by neutral-surface folding. The *x*-axis is parallel to the folded surface in the outer arc and perpendicular to this surface in the inner arc. Yet the magnitude of the strain ratios predicted by neutral-surface folding is too low in the natural pattern, so the pattern requires additional modification to match the natural fold. One solution is shown in Figure 10.37b, where prefolding compaction (nonconstant volume, layer-perpendicular shortening) is followed by neutral-surface folding, during which material is preferentially removed from the inner arc. Dissolution and material transport during folding are quite common in natural rocks. Quartz and calcite veins in folded rocks are examples of this transport. Other natural folds show that flexural folding and shear folding are the dominant mechanisms, so all our folding models offer reasonable first-order approximations to the inner workings of a folded layer.

The example in Figure 10.37 emphasizes that strain in folds is highly heterogeneous, but we can nonetheless estimate the bulk shortening strain from the fold shape by adapting Equation 4.1. The bulk strain is given by

$$\mathbf{e} = (W - L)/L \qquad \text{Eq. 10.7}$$

where L is the arc length and W is the wavelength. Applying this to our example we obtain a value for **e** of approximately –0.35, or ~35% bulk-shortening strain.[18]

10.9 A POSSIBLE SEQUENCE OF EVENTS

We close the chapter on folding by an interpretive sequence of events in the formation of a single-layer fold. Immediately follow-

[18]If compaction does not lengthen the layer, this longitudinal strain estimate is tectonic strain.

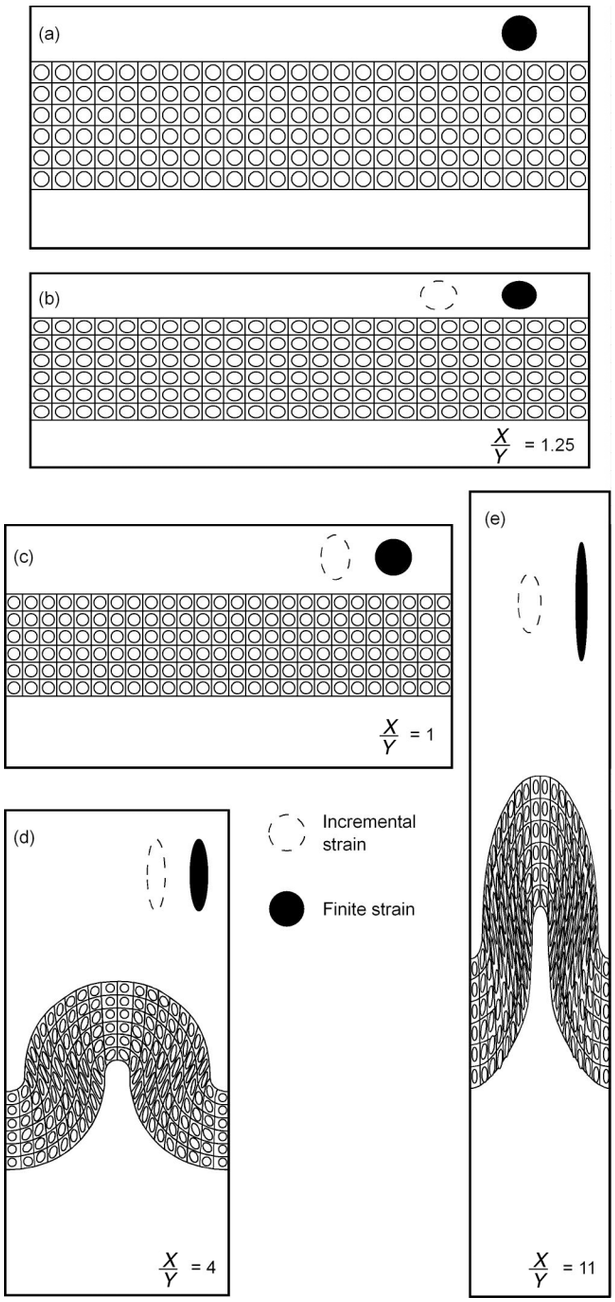

FIGURE 10.38 Folding scenario with the corresponding strain states at each step. An initial layer (a) undergoes 20% compaction (b). This is followed by layer-parallel shortening (c) and buckling (d). The final stage is a homogeneous shortening strain which transforms the parallel fold into a similar fold. The finite strain in the layer is indicated at each step; the incremental strain (dashed) and finite strain (solid) ellipses of the system are shown in the upper right. Strain ratios are shown for each step. It is assumed that volume loss occurs only at the compaction stage (b).

ing deposition of the bed, compaction reduces its thickness. We use an intermediate value of 20% layer-perpendicular shortening strain for this first component in our example (i.e., $X_c/Z_c = 1.25$), which represents 20% area loss (Figure 10.38b); in nature, compactional strains range from 0% to 50%. During the first stage of buckling, the competent layer changes dimensions by layer-parallel shortening (lps). You recall that layer thickening is more important at low viscosity ratios, so in our example we assume 20% layer-parallel shortening. This constant-volume, homogeneous strain component (conveniently) restores the finite strain ellipse to a circle ($X_f/Z_f = 1$), but the corresponding lps strain ratio X_{lps}/Z_{lps} is 1.25 (Figure 10.38c). Continued shortening results in the initiation and growth of a parallel fold by flexural folding, with a characteristic arc length (L) as a function of the thickness (t) of the layer and the linear viscosity ratio (η_L/η_M). We can estimate the viscosity ratio of the system by measuring the ratio L/t and the strain ratio X_{lps}/Z_{lps} of the layer. Until this buckling stage, the strain has been homogeneous, but after fold initiation the strain is heterogeneous, with coaxial strain dominating the hinge area and non-coaxial strain dominating in the limbs of the fold (Figure 10.38d). The bulk finite strain of the system is represented by the ratio X_b/Z_b (i.e., 4). When resistance to further folding has been reached, continued shortening is achieved by superimposed homogeneous strain (Figure 10.38e). The end result of these stages produces a similar fold with a strain pattern that varies as a function of the degree of compactional strain, the operative fold mechanism, the viscosity ratio, and the degree of superimposed homogeneous strain. The finite strain ratio X_f/Z_f for our history is 11, which corresponds to a total layer-parallel shortening strain of ~70%.

One can vary this scenario in many ways by simply changing the values of the strain ratio at each step, but also by introducing volume loss during the stages of buckling and superimposed homogeneous strain. Examining alternative scenarios will give you a good idea of folding and strain distributions under different conditions; modern imaging programs for personal computers offer a simple way to experiment. For example, in metamorphic rocks there is little competency contrast between the layers, and layer-parallel thickening may be much more important than in low-grade sedimentary beds. Moreover, elevated temperature conditions promote grain dissolution and transport of material. It is therefore particularly instructive to examine the history of a system experiencing 50%

FIGURE 10.39 Large recumbent fold in Nagelhorn, Switzerland, showing the characteristic nappe style of deformation in this part of the European Alps.

volume loss ($\Delta = -0.5$) during the buckling and superimposed homogeneous strain stages. This represents a geologically reasonable condition we will return to in the chapter on rock fabrics (Chapter 11).

10.10 CLOSING REMARKS

Hopefully you did not lose sight of the natural beauty of folds after learning so much about description, terminology, and mechanics. Folds are simply fascinating to look at, and the bigger the better (Figure 10.39). We study them to understand the conditions and significance of deformed rocks and regions. Folding patterns are good representations of the orientation of regional strain, and we can follow regional strain changes with time through the analysis of fold superposition. Superposed folding presents a particular challenge that awakens the puzzler in us. Fold generations should be based only on fold superimposition patterns, perhaps aided by fold style for correlation between outcrops. As a "tongue-in-cheek" rule, the number of fold generations should always be much less than the number of folds you have encountered in the field.

Folds are strain indicators, but the mechanical contrast between neighboring layers and with the matrix implies that strain data is representative of the folded layer, and not necessarily of the bulk rock. This is not a crippling limitation for regional analysis, nor is the problem unique to folds; it holds for all strain markers. Strain within a fold is markedly heterogeneous and the local pattern may be very different from regional conditions. The relationship of folds to regional stress is even less straightforward because of the mechanical interaction between layers with contrasting competency. Nonetheless, in many circumstances, folds may also tell us about these and other rheologic properties of rocks.

Although most of this chapter focuses on single-layer folding, the material should give you sufficient insight to tackle the literature on multilayer systems and other advanced topics on folding (such as nonlinear material rheologies). You are hopefully itching to go out into the field and test some of these concepts and ideas; otherwise a few additional laboratory experiments may satisfy your appetite until summer comes around. Finally, you will find that folds are commonly associated with other structural fabrics, such as foliations and lineations; these features are the topic of the next chapter.

ADDITIONAL READING

Biot, M. A., 1961. Theory of folding of stratified viscoelastic media and its implication in tectonics and orogenesis. *Geological Society of America Bulletin,* 72, 1595–1620.

Currie, J. B., Patnode, H. W., and Trump, R. P., 1962. Development of folds in sedimentary strata. *Geological Society of America Bulletin,*73, 655–674.

Dietrich, J. H., 1970. Computer experiments on mechanics of finite amplitude folds. *Canadian Journal of Earth Sciences,* 7, 467–476.

Hudleston, P. J., and Lan, L., 1993. Information from fold shapes. *Journal of Structural Geology,* 15, 253–264.

Latham, J., 1985. A numerical investigation and geological discussion of the relationship between folding, kinking and faulting. *Journal of Structural Geology,* 7, 237–249.

Price, N. J., and Cosgrove, J. W., 1990. *Analysis of geological structures.* Cambridge University Press: Cambridge.

Ramberg, H., 1963. Strain distribution and geometry of folds. *Bulletin of the Geological Institute, University of Uppsala,* 42, 1–20.

Ramsay, J. G., and Huber, M. I., 1987. *The techniques of modern structural geology, volume 2: folds and fractures.* Academic Press.

Sherwin, J., and Chapple, W. M., 1968. Wavelengths of single layer folds: a comparison between theory and observation. *American Journal of Science,* 266, 167–179.

Thiessen, R. L., and Means, W. D., 1980. Classification of fold interference patterns: a reexamination. *Journal of Structural Geology,* 2, 311–316.